12-2013

Development of Novel Subunit Vaccine against H5N1 Influenza

Lu Zhang
University of Arkansas, Fayetteville

Development of a Novel Subunit Vaccine against H5N1 Influenza

Development of a Novel Subunit Vaccine against H5N1 Influenza

A thesis submitted in partial fulfillment
Of the requirements for the degree of
Master of Science in Cell and Molecular Biology

by

Lu Zhang
Fudan University
Bachelor of Science in Biological Sciences, 2010

December 2013
University of Arkansas

This thesis is approved for recommendation to the Graduate Council.

Dr. Kaiming Ye
Thesis Director

Dr. Douglas Duane Rhoads
Committee Member

Dr. Sha Jin
Committee Member

ABSTRACT

Influenza is a common infectious disease resulting from a frequently mutated RNA virus. Vaccination is currently the most effective method to prevent people from seasonal or pandemic influenza. The production of traditional egg-based influenza vaccine is time-consuming and provides limited effect against new strains. Therefore, it is necessary to develop a rapid method to produce influenza vaccines. We proposed a novel influenza vaccine based on the *E.coli* expression system. Hemagglutinin (HA) is the major target surface protein of influenza virus for vaccine development. In this study, we sub-cloned the HAs encoding gene into an *E. coli* expression vector; the signal peptide sequence, the transmembrane and cytoplasmic domains of the whole HA of H5N1 (A/Vietnam/1203/2004) were removed. Expression of recombinant HAs fused with a C-terminal His-tag was investigated and confirmed through SDS-PAGE and Western blot assay. After being purified under denaturing conditions using NTA-Ni affinity chromatography, HAs were dialyzed for refolding. We obtained concentrated recombinant HAs from bacterial cultures at a yield of 250 μg/ 500 ml. Finally, animal studies revealed the production of anti-HA antibodies in mice immunized with different doses of the recombinant HAs. We also compared the adjuvant effects of iron oxide nanoparticle (IONs) and selected commercial adjuvants. These results suggest that this system has the potential to be a new method for the mass production of influenza vaccines at low cost. More efforts are going to be focused on the adjuvant effect of IONs in future work.

ACKNOWLEDGEMENTS

First of all, I would like to express my greatest gratitude to my advisors Dr. Kaiming Ye and Dr. Sha Jin for providing an excellent lab environment and support throughout my whole study period. Their rigorous and motivating attitudes towards research influenced me and encouraged me to overcome difficulties in my study as well as in my life. They especially offered me a large degree of freedom to be trained as an independent researcher.

I would also like to give sincere thanks to Dr. Douglas Duane Rhoads for his help with this thesis and support from the CEMB program; thanks to Stacy Leann Sanchez, Kelli Nixon and Shannon G. Davis for their support from the Department of Biomedical Engineering. Special thanks go to Drs. Gisela Erf, Robert Beitle and Christa Hestekin for their guide and suggestion during my program study. It would be impossible to make it through the semester without the help from all these people.

I want to thank Drs. Hong Xu and Hongyu Chen from Ocean Nanotech, LLC for preparing the iron oxide nanoparticles coating with NTA-Ni which were investigated in this study. Thanks are also due to Carol A. Rodlun from CLAF at the University of Arkansas for reviewing the IACUC protocol and taking care of the animals used in this study. I would like to thank Drs. Lingyun Zhou, Han Lei, Qing-Long Liang and Yu Wen who guided me in the experiment design and practice. I also appreciated technical help with animal injections from Bhanu Prasanth Koppolu.

I am thankful to my lab members Weiwei Wang, Yarina Masniuk, Jon Earls, Ngoc Thien Lam, Pantrika Krisanarungson, Hanan Al-Tyair, Huantong Yao and other friends in the department and Fayetteville for their precious solicitude and company during the past few years.

DEDICATION

This thesis is dedicated to my parents Yue and Li, who suffered from our geographic separation for years and always quietly supported me from China. It is also dedicated to Bronson and Evelyn Stilwell, my American parents in Fayetteville, AR, who gave me the warmest care and friendship for the past years.

TABLE OF CONTENTS

I. INTRODUCTION

1.1 Influenza

1.1.1 Influenza virus

Influenza, usually known as 'the flu', is an infectious disease resulting from a RNA virus of the family of *Orthomyxoviridae*. The influenza viruses can cause influenza in many species of vertebrates including birds, humans and other mammals. In humans, it is typically transmitted through the air by coughs or sneezes, by direct contact with bird droppings or nasal secretions, or by contact with contaminated surfaces. The classic symptoms of influenza include fever, myalgia, sore throat, nonproductive coughing and headache. Additional symptoms may appear such as runny nose, eye pain and substernal chest burning (1).

There are three immunologic types of the influenza virus: Type A, Type B and Type C. Although wild aquatic birds are the natural carriers of various Type A influenza viruses (2), this kind of influenza virus occasionally transmits to other species and causes pandemics. Both Type B and Type C viruses are less common then Type A influenza viruses. Type B only infects humans, seals and ferrets, while Type C only infects humans, dogs and pigs. Among these three genera of influenza viruses, Type A virus is considered as the most virulent human pathogens (3).

Based on the antibody response to these viruses, the influenza viruses could be further subdivided into different serotypes. Influenza A viruses are classified by their two surface antigens: Hemagglutinin (HA) and Neuraminidase (NA) (4). Up to now, 16 HA subtypes (H1-H16) and 9 NA subtypes (N1-N9) have been identified. The virion, the entire virus particle, is commonly roughly spherical and about 80-120nm in diameter. Their ultrastructural details can be depicted by the negative-stained transmission electron microscopy (TEM), as shown in Fig. 1.1(A). The nomenclature of the influenza viruses is expressed in this order: 1) virus type, 2) the

first geographic site where it was isolated, 3) strain number, 4) year of isolation, and 5) subtype of virus (Fig. 1.1[B]). For example, the antigen produced in this study is from genomes of A/Vietnam/1203/2004(H5N1), and it is an H5N1 influenza A virus which was first isolated from Vietnam in 2004.

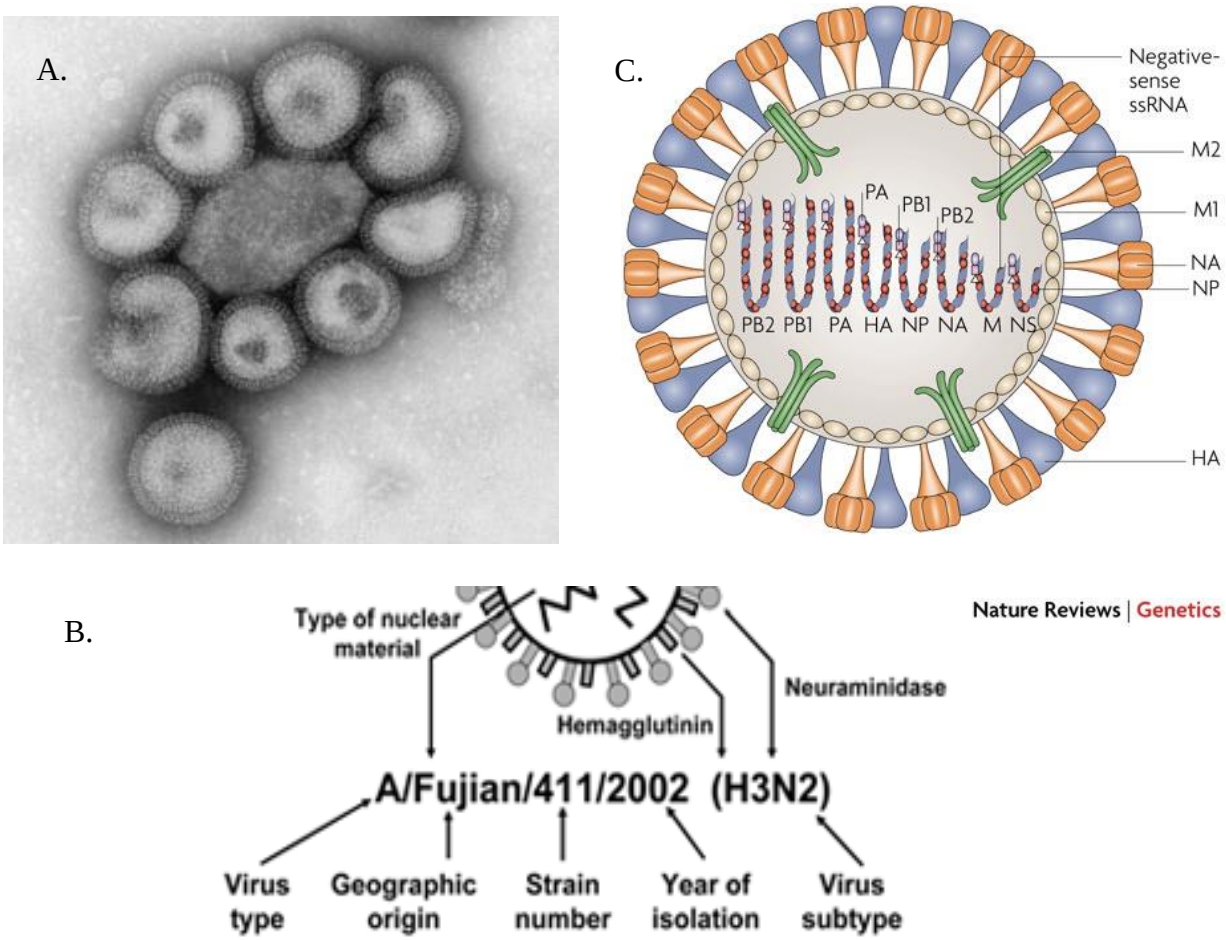

Fig. 1.1 A. Electron microscopy images of influenza viruses (67)**. B. Nomenclature of influenza viruses** (1)**. C. The molecular structure of influenza A virus.** Figure is adapted by permission from Macmillan Publishers Ltd: [Nature Reviews Genetics] (65), copyright (2007).

The molecular structures of the three different types of influenza viruses are similar. As shown in Fig. 1.1(C), the Influenza A viral envelope is wrapped with spikes of two main glycoproteins: HA and NA. In the central core are the viral RNA genome and other viral proteins. The RNA genome consists of eight pieces of segmented negative-sense RNA, each containing one or two

genes. These RNA segments encode eleven proteins: HA, NA, nucleoprotein (NP), matrix protein M1 and M2, nonstructural protein NS1 and NS2, and polymerase subunit PA, PB1 and PB2. Previous research revealed that four of these proteins: HA, NA, NP and M1 are the important targets of host immune response. Because NP and M1 proteins are located inside the virus, the humoral and cellular responses they elicit cannot neutralize the virus. Therefore, HA and NA are the prime candidate antigens for developing influenza vaccine (5).

1.1.2 Characteristics of Hemagglutinin

HA is a trimeric protein composed of three monomers; HA1, HA2, and HA3 domains. The trimeric protein is divided along the longitudinal axis of the protein to a globular domain and a stem domain. As shown in Fig. 1.2, the beta-sheets are primarily present in the globular domain where the binding region to sialic acid locates, while the stem region of the HA is made of the alpha helices.

The full length HA gene sequence consists of signal peptide, two subunits: HA1 and HA2, transmembrane polypeptide and cytoplasmic domain. In this study, we removed the amino-terminal 16 bp signal peptide, the transmembrane polypeptide and cytoplasmic domain at its C terminus to avoid targeting after protein translation. Thus, the calculated molecular weight of the truncated HAs monomer in influenza A virus A/Vietnam/1203/04 (H5N1) is 58.7 kDa with an isoelectric point of 6.59 based on the protein sequence using online calculator (6).

As the most abundant surface glycoproteins of influenza virus, HA has been recognized as a key antigen in the host response to the influenza virus in both natural infection and vaccination. The main function of HA is to mediate the binding of virus to target cells and the entry of the viral genome into the target cells (2). Upon HA’s binding to the sialic acid sugars on the surfaces of

epithelial cells in the nose, throat, lungs of mammals and intestines of birds, the virus enters the target cell by endocytosis. HA is one of the main determinants of the host range of influenza A viruses due to its specificity for receptor recognition and binding. Moreover, conserved insertions of peptides adjacent to the cleavage site between HA1 and HA2 were found in several highly pathogenic avian A viruses H5N1. HA is also important to determine the virulence of avian influenza A viruses in poultry (7). Among different subtypes, H5 and H7 have a highly cleavable HA so that they may infect humans and result in pandemics (5).

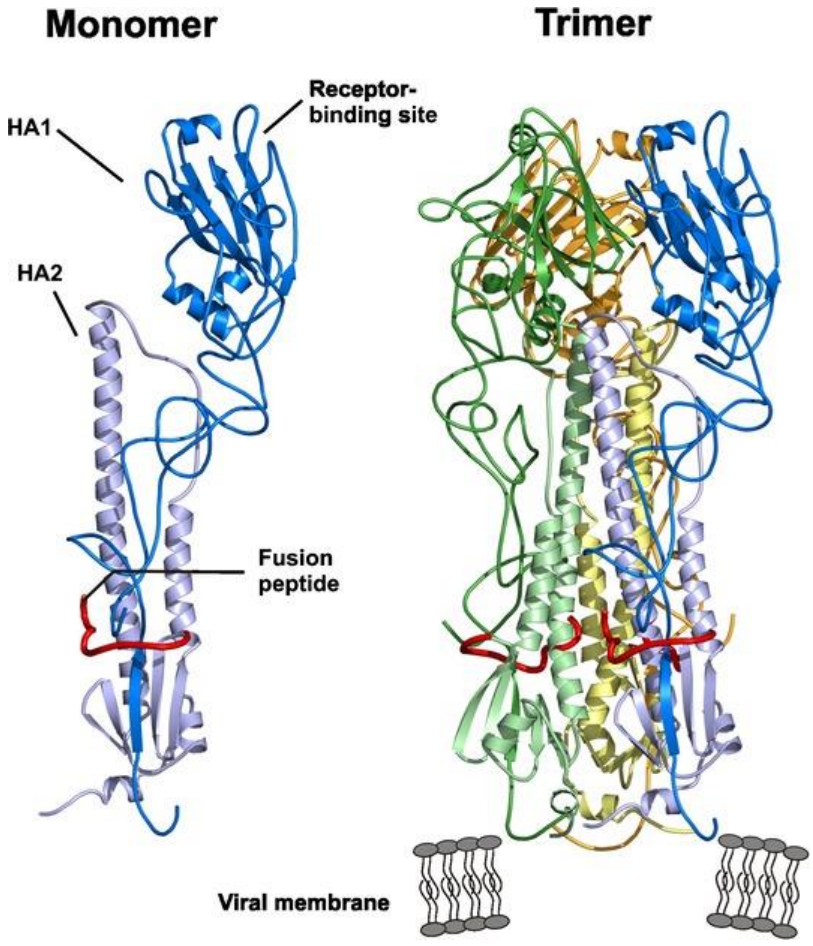

Fig. 1.2. The three-dimensional structure of the influenza HA monomer and trimer. Figure was made by André van Eerde (University of Groningen), using MOLSCRIPT, according to file from Protein Data Bank, code 3HMG (68).

1.1.3 Influenza pandemic

In the 20th century, four influenza pandemics occurred and each resulted from new strain of the virus in humans. The 1918 ‘Spanish influenza’ H1N1 virus which originated from an avian virus adapted to transmit efficiently in humans. It resulted in such a severe pandemic that the total deaths were estimated at approximately 50 million in a worldwide range (8). Besides, all the other pandemics were related to this H1N1 virus. The mechanisms of the origination of the first three pandemics are presented in Fig. 1.3. The reassortment of 1918 H1N1 and other avian viruses led to the 1957 ‘Asian influenza’ H2N2 virus and 1958 ‘Hong Kong influenza’ H3N2 virus, separately. The latest pandemic influenza happened in 2009 (subtype A/H1N1).

In order to circumvent the immune responses of the host animals, the viral genomes mutate frequently. Usually, the sites on HA and NA proteins that are recognized by the host immune system are under constant selective pressure. The variation of influenza viruses, which are due to antigenic drift (mutations on HA and NA) and/or antigenic shift (re-assortment of the subtypes of viral gene segments), could cause an influenza epidemic or pandemic if the population has no inherent immunity against the new strain. New influenza strains appear 1) when existing viruses in other species adapt to human hosts; 2) existing human viruses genetically re-assort genes from viruses which usually infects birds or pigs. For example, the 2009 H1N1 is a novel influenza virus that combines genes from human, swine and bird flu viruses. A pandemic of influenza may begin with isolated cases, exploding when the virus evolves the ability to transmit efficiently in humans.

H5N1, the focus of this study, is a highly pathogenic avian influenza virus which resulted in severe disease with high morbidity and mortality, devastating poultry industries worldwide. Generally, people are not susceptible to be infected by H5N1, but mutated viruses started to

infect humans and cause severe diseases and death. As early as 1997, an avian H5N1virus (A/Hong Kong/156/97) was isolated from a three-year-old boy with a fatal illness consistent with influenza in Hong Kong. Molecular analysis of the gene segments showed that the H5 in this strain was from a turkey influenza virus in 1991 (7). Six of eighteen individuals died since the first report of the human H5N1 infection. The virus temporarily disappeared in human population but remained in birds in South East Asia until it recurred in humans in 2003 and 2004. Cases that infect humans were thought to be brought from close contact with poultry, while the first account of probable human-to-human transmission was published Jan 2005 documenting a mother in Thailand who probably contracted virus from her daughter in Sep 2004 (9) . From 2003 to the writing of this thesis (Oct 2013), H5N1 has resulted in 641 WHO-confirmed infections and 380 deaths with a mortality rate of 59.3% (10).

Concerns were raised whether large amounts of funds should be provided to research developing vaccines against H5N1 since it has limited transmission among humans (11). For short-term interests, it is true that research funds need to be invested on researches on other more devastating diseases. However, in a long-term view, this highly pathogenic virus is one of the candidate viruses for pandemic preparedness (12). WHO data mentioned above already showed the high morbidity and mortality rates brought from the H5N1 infection in humans. Though most of them bring seasonal infections with light symptoms in humans, it is never wise to underestimate the potential impact of new strains. During its geographic spread, the H5N1 virus underwent antigenic drift and/or shift as all other influenza viruses (13). Since the H5N1, H1N1 and other subtype of influenza virus coexist in the same environment, we must give more attention to the risk of potential pandemic spread. Considering that the viruses mutate rapidly, researchers should maintain their interest in improving pandemic influenza vaccines despite the

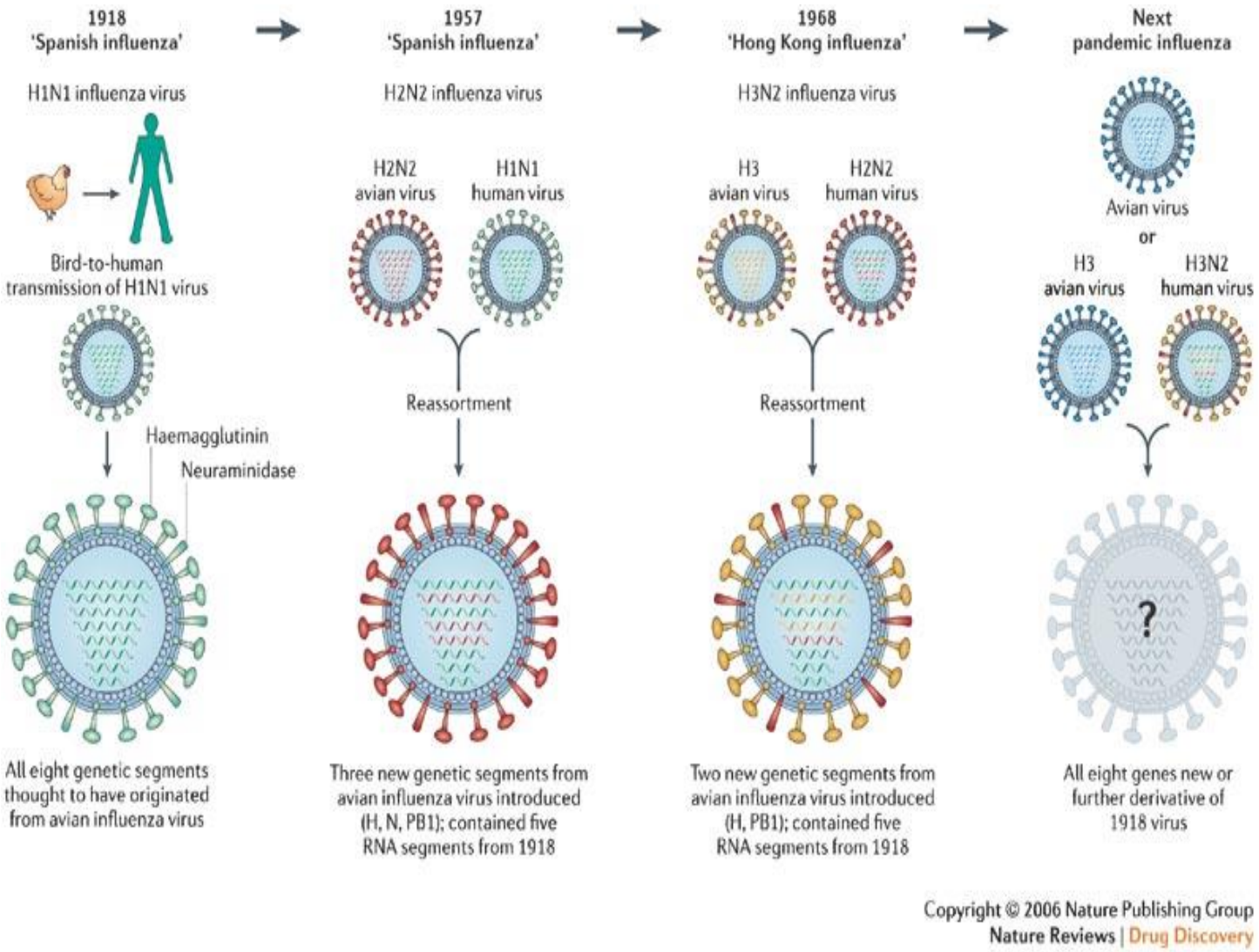

Fig. 1.3. The mechanism by which pandemic influenza originates in 20th century. Figure is adapted by permission from Macmillan Publishers Ltd: [Nature Reviews Drug Discovery] (62), copyright (2006) from (63).

fact that public concern has subsided. We have reason to believe that if the H5N1 virus picks up the capability to transmit among humans, it may cause a worse pandemic than 1918 Spanish flu.

1.2 Development of Influenza vaccination

1.2.1 Traditional egg-based vaccines

Vaccine, antiviral drugs and personal preventive care are the common methods for influenza prevention. Among them, vaccination of public is the most effective way to combat influenza. Embryonated eggs have been employed in the production of influenza virus since 1937, because they can produce large amounts of virus to be processed to inactivated vaccines in a safe and relatively low cost method (14). The inactivated vaccines consist of whole inactivated virus, detergent-split virus or purified HA and NA subunits. Currently, the most common vaccine used against the seasonal influenza is the trivalent influenza vaccine (TIV) that contains inactivated antigens from two influenza A virus strains and one influenza B virus strain. The three influenza strains selected by WHO are propagated in chicken eggs, chemically inactivated and semi-purified (15). An alternative approach is the live-attenuated influenza vaccines (LAIV) based on a cold-adapted and temperature sensitive virus (16). They are also cultured in eggs but administrated by nasal spray.

The major limitations of these egg-based vaccines are the long production time and requirements for large amounts of eggs (Table 1.1). Because natural viruses are usually not able to grow well in eggs, re-assortment of genes between the new virus strain and an egg-adapted strain such as A/Puerto Rico/8/34(PR8) (H1N1) is required through traditional or reverse genetics technology. It may take up to ten months to screen a suitable candidate virus for vaccine due to the variety of production yield of different strains. Even though these egg-based vaccines are effective to the annual seasonal influenza with the predicted strain, the speed to produce them is far from rapid

enough to fight any sudden breakout of pandemic strain. On the other hand, this method does not work for viruses that are lethal to chicken embryos such as H5N1 strain (17). Also, individuals who are allergic to egg cannot accept vaccine produced by this method.

The incapability of worldwide-scale production is another challenge for influenza vaccine development. The gap between the expected demands for future pandemic influenza vaccines and global production capacity need to be bridged (14). Obstacles such as high cost, troublesome distribution and administration logistics of current flu vaccines are the main reasons that prevent people in developing countries from receiving vaccination. Thus, it is essential to develop new technologies to realize rapid, massive and low cost production of influenza vaccines.

1.2.2 Development of novel vaccines using new technologies

Due to the limitations of egg-based vaccines, other approaches have been studied to replace them. One approach is to develop culture-based vaccines. The influenza viruses are cultured in cell-filled bioreactors that do not rely on the maintenance of huge flocks of chickens; this may result in a shortened production period. Up to now, efforts have been made to produce influenza vaccine using Vero, Madin-Darby canine kidney (MDCK) or PERC.6 cell-cultures (14). Among them, MDCK cells are most suitable for production of influenza viruses in serum-free media. Drug safety studies showed that the MDCK cell line is safe for biological production (18) and Phase I clinical trials showed that split vaccines derived from cell culture is highly immunogenic in adults (19). Another group compared formalin-inactivated influenza B virus vaccines propagated in different host system and showed that the cell-culture based vaccines were as effective as egg-based vaccines (20). Currently, Sanofi Pasteur, Novartis and Solvay produce mammalian cell culture influenza vaccines licensed in Europe or in the US (16). However, cell culture systems have drawbacks such as the difficulty in scale-up production and occasional

contamination. Also, the application of mammalian cell lines may introduce specific mutations which result in structural changes of the antigen, which in turn diminishes the efficacy of the vaccines (21; 22).

DNA vaccination is a promising vaccine technology. It is easy to manipulate: simply inject small genetically engineered DNA encoding the antigen instead of using the antigen itself. One of its advantages is the fast production and ease of storage. DNA vaccines against new influenza strains can be produced in weeks, rather than months, and the vaccine stock can last years without refrigeration. In addition, studies showed that DNA vaccines induce both major histocompatibility complex (MHC) class I and II responses (23) and long- term humoral and cellular immune responses (24). As for DNA influenza vaccines, one encoding HA protein was exhibited to be safe and immunogenic by intramuscular and intradermal routes in humans in phase I clinical studies (25). The possibility of foreign gene integration to the host genome is a major concern about this type of vaccine. Also more clinical studies are needed to investigate the efficacy of DNA vaccines in humans.

Another approach of egg-free influenza vaccine production is the development of recombinant protein (antigen)-based vaccines. The development of recombinant DNA technology realized the expression of viral proteins as antigens in the vaccine formulations, which are safer than the vaccines that use live, attenuated or killed pathogens. Moreover, it is easy to achieve rapid and massive production of proteins followed by purification and distribution. Several kinds of expression systems have been applied to express HA molecule from the influenza virus such as adenoviral virus (26) and baculovirus system (15). A recombinant multimeric H5 hemagglutinin protein (rH5) was successfully produced using a baculovirus expression vector system in SF+

Egg-based vaccine	
Advantages	• Safe, effective and relatively low cost
Limitations	• Screening of desirable virus strains is needed in advance • Lengthy manufacturing process: up to ten months • Rely on the maintenance of huge flocks of chickens • Not available for viruses which are lethal to chicken embryo • Not available for individuals with egg allergy
Cell culture-based vaccine	
Advantages	• Cultured in bioreactor , easier to handle • safe and as effective as egg-based vaccines
Limitations	• High-yielding re-assorted virus is needed • Difficulty in scale-up production • Cell line specific mutations which results in antigenic and structural changes of the HA protein may be introduced • Cross-contamination may occur during manufacturing process
Recombinant protein (antigen)-based vaccine	
Advantages	• Recombinant DNA technology is applied to produce the viral proteins • The antigens are purified and utilized as the active ingredients in vaccine
Limitations	• Weak immunogenicity

Table 1.1. Comparation of different methods to produce influenza vaccine

insect cells (27). A virus-like particle (VLP) vaccine manufactured in Sf9 insect cells was evaluated by their humoral immune response in humans in an FDA-approved phase I/II clinical study (28). *E.coli* expression system is a mature system applied in the production of recombinant proteins. This is also an attractive system in influenza vaccine production because it provides fast, low cost and massive production of antigens. The doubling time of *E.coli* cells is as short as 20 min, and up to 50% of the recombinant proteins locate in inclusion bodies which are easy to collect for purification. For decades, the correct folding, glycosylation and secretion of HA has

always been considered necessary for HA production in vaccine development. However, studies showed that the bacteria system without posttranslational modification could be used to produce effective influenza vaccines. Hana Golding and her team developed a bacterial system to express and purify properly folded globular domain HA1 of H5N1 which is immunogenic in mice and ferrets. Moreover, they first identified a functional N-terminal oligomerization sequence in HA1 (29). The important obstacle to the development of antigen-based vaccine is the weak immunogenicity of the recombinant antigen protein. Although recombinant DNA technology allows fast and massive production of a single antigen, the immunogenicity of the antigen is usually limited. Accordingly, large antigen doses or repeat administration are required to produce an adequate immune response. To solve this problem, some vaccine additives have been investigated to combine with these antigens to maximize immunogenicity and manufacturing capacity.

Considering that the current influenza vaccine needs to be updated every year to adapt to the antigenicity of the virus strains that are predicted to circulate in the next flu season, they will not be able to provide effective protection during the emergence of a novel strain of pandemic influenza virus. Therefore, efforts have been focused to develop a broadly cross-protective vaccine, known as ‘universal’ vaccines. Approaches are targeted at the conserved proteins such as the external domain of the influenza M2 ion channel protein and HA fusion peptides and stalk domains, but most studies are at the level of animal models (30).

1.2.3 Adjuvants in influenza vaccines

During the development of an influenza vaccine, it is essential to evaluate its safety and immunogenicity in special groups such as infants, pregnant women, immuno-compromised individuals or people over 65 years old. For example, the standard TIV offers relatively poor

efficacy for people over 65, the fastest-growing group in our population who suffer greater morbidity and mortality than the young when infected by influenza. Aging is related to decline in immune system functions, which results in less robust innate and adaptive immunity. Instead of increasing the dosage or number of immunizations, the addition of other components might induce a protective and long-lasting immune response.

Adjuvants are such vaccine additives that act to accelerate, prolong or enhance antigen-specific immune responses when combined with the antigens (31). Products with effective adjuvant may benefit newborns, the elderly or immuno-compromised people (32). The word "adjuvant" comes from the Latin word "Adjuvare" which means "to help" (33). The adjuvant itself should cause no or minimal toxicity or immune effects. There are two classes of adjuvants applied in modern vaccine development (Table 1.2.). Immunostimulants mimick structures of evolutionarily conserved molecules, such as components of bacterial cell walls, endocytosed nucleic acids such as dsRNA, ssDNA, and unmethylated CpG DNA *etc* (34). These substances are also named pathogen-associated molecular patterns (PAMPs). Once antigens are combined with these adjuvants, cells in innate immune response systems, including dendritic cells (DCs), lymphocytes and macrophages will be activated as if attacked by a natural infection. Another type of adjuvant is a vehicle that presents the antigens to the immune system via controlled antigen release and depot delivery systems.

Alum, referred to as aluminum salt based adjuvants, is one of the adjuvants in approved human vaccines. The antigens are adsorbed onto highly charged aluminum particles to formulate the vaccines. Alum adjuvants have been developed to elicit protective antibody responses. Their advantages include safety, simple formulation for large production, together with their capacity to augment the humoral responses by providing Th2 cells help to follicular B cells (35).

Meanwhile, alum adjuvants are limited in that they are not able to elicit cell-mediated Th1 or CTL responses against intracellular pathogens (36). Its inability to be frozen is another disadvantage.

Oil-in-water (o/w) emulsions are other adjuvants applied in human vaccines. They are advanced to increase the breadth of cross-reactive antibodies and possess significant dose-sparing activity. Addition of oil-water based emulsion adjuvants offer a 4-fold dose sparing effect on standard egg-based vaccine (16). MF59^{TM}, consisting of an o/w emulsion is used in Europe as an adjuvant in influenza vaccines. It improves the immune response to a H5N1 vaccine by inducing qualitative and quantitative expansion of the antibody repertoires with protective potential (37). Although it does not induce increased CD4+ Th1 immune responses like alum, it has the potential to be applied in influenza vaccines due to its capacity to increase the hemagglutination inhibiting antibodies and CD8+T-cell responses (38). Novartis developed Aflunov, an egg-derived, subunit vaccine which received the approval from the Committee for Medicinal Products for Human use (CHMP) in adults aged above 18 years in September 2010. This pre-pandemic vaccine consists of 7.5 µg HA from the avian A/H5N1 virus and adjuvant MF59. Studies have revealed that it meets the requirements for pre-pandemic vaccine: safety, ability to induce broad cross-neutralizing antibody response and ability to induce strong and long-lasting immunological memory (13).

It is paramount to the effectiveness of adjuvants to activate DCs which results in enhanced presentation of the antigenic peptides on MHC class I and II to the TCR. A leading adjuvant targeting DC is the family of innate Toll-like receptors, particularly the LPS receptor, Toll-like receptor 4 (TLR4). TRIA Bioscience Corp. and protein Sciences Corp. are working on GLA-SE, a two-part adjuvant system comprised of glucopyranosyl lipid adjuvant (GLA), a formulated

synthetic TLR4 agonist, and a stable emulsion (SE) of o/w. This adjuvant together with recombinant HA was demonstrated to protect mice and ferrets against a high titer challenge with H5N1 virus. They successfully augment neutralizing antibody titers via Th1-mediated antibody responses (39).

Current researchers usually focus on studies of antigens at the same time testing the antigens

Immunostimulant	Cellular interaction	Type of immune response
TLR ligands		
Bacterial lipopeptide, lipoprotein and lipoteichoic acid; mycobacterial lipoglycan; yeast zymosan, porin	TLR-2, 1/2, 2/6	Th1, antibody (Ab), NK cell
Viral double stranded RNA	TLR-3	NK cell
Lipopolysaccharide, Lipid A, monophosphoryl lipid A (MPL®), AGPs	TLR-4	Strong Th1, Ab
Flagellin	TLR-5	Th1, CTL, Ab
Viral single stranded RNA, imidazoquinolines	TLR-7/8	Strong Th1, CTL
Bacterial DNA, CpG DNA, hemozoin	TLR-9	Strong Th1, CTL and Ab; NK cell
Uropathogenic bacteria, protozoan profilin	TLR-11	Th1
Other		
Saponins (Quil-A, QS-21, Tomatine, ISCOM, ISCOMATRIX™)	Antigen processing	Strong Th1, CTL and Ab; long term memory
Cytokines: GM-CSF, IL-2, IFN-γ, Flt-3.	Cytokine receptors	Th1, Ab
Bacterial toxins (CT, LT)	ADP ribosylating factors	Ab

Vehicle or delivery systems	Type of immune response					
	Th1 responses	Th2 responses	Cross priming	B-cell responses	Mucosal responses	Persistent T- and B-cell responses
Mineral Salts (aluminium salts, calcium phosphate, AS04 [Alum+MPL®])	+	++	–	+++	–	+
Emulsions [MF59™ (squalene/water), QS21, AS02 (squalene+MPL®+QS21), IFA, Montanide®, ISA51, Montanide®, ISA720]	++	–	–	+++	–	–
Liposomes (DMPC/Chol, AS01)	+++		+	+	–	+
Virosomes (IRIV), ISCOMs	++	++	++	+++	–	–
DC Chol, mineral oil, IFA, Montanide®, squalene	–	++	–	+++	–	–
Mucosal delivery systems: Chitosan	–	–	–	–	–	++
Microspheres	+	–	++		–	–

Table 1.2. Immune responses triggered by immunostimulants and vehicles or delivery systems. Adapted from (36).

with several adjuvants. It seems that no single adjuvant can produce broad and long-lasting immune responses that are required for all new vaccines. Challenges remain regarding how to develop novel adjuvants as well as how to standardize the adjuvants formulated in different laboratories or companies.

1.3 Nanoparticles and their application in biomedical engineering

1.3.1 Nanoparticles

Without an international definition, nano-particles (NPs) usually refer to the particles with size smaller than 100 nm. Engineered NPs have been used to provide diagnostic, therapeutic and prognostic information about the status of disease. They are ideal for antigen delivery for several reasons. 1) Based on their high surface ratio, function groups can be added on their surface to attach target reagents. 2) Their hydrodynamic size from 10-100nm could prevent their elimination from blood by kidney or liver. 3) Their near-neutral zeta-potential could minimize the nonspecific interaction with blood components. 4) They are highly stable in physiologically relevant media (40). Therefore, NPs are potential vaccine delivery platforms or adjuvants for vaccine development.

Because their size is comparable to pathogens, NPs can be efficiently recognized by immune cells and facilitate the delivery of antigens to antigen presenting cells (APCs). Different strategies to design NPs targeting DCs are described in Fig. 1.4, as DCs, the major APCs, play important role in both innate and adaptive immune responses. The antigen can be attached to the surface of NPs via chemical or physical interaction; the antigen can also be encapsulated inside the nanoparticles so that it is protected from degradation. Additionally, NPs can combine with biological molecules as address labels to guide vaccines to specific sites *in vivo* (41; 42; 43).

1.3.2 Current application of NPs in vaccination

NPs have been widely applied in vaccine development due to the advantage of their small size, high drug-loading capacity, controllable drug release, *etc* (44). NPs can be broadly classified into three categories: liposomes, polymers, and inorganic nanomaterials (45). Those applied in vaccine approaches include liposomes, nano-emulsions, polymeric NPs, dendrimers and immunostimulatory complexes (ISCOM) (46). Lipid polymers PLGA have been applied to delivery Hepatitis B virus (HBV) surface antigen (47) and fusion peptide and GM-CSF DNA (48). Self-assembling protein nanoparticle (SPAN) was used for peptide sporozoite malaria vaccine (49).

Approaches to the application of NPs as biomedical vehicles face many challenges. NPs can be removed by phagocyte cells. The NPs carrying antigens can be degraded if they cannot move out of endosome. For those antigens which are encapsulated inside NPs, their antigenicity might be destroyed during the encapsulation process. To delay the macrophage-mediated clearance of NPs, a group of researchers fused 'self-peptides' CD47 to the NPs to pretend that these NPs are self-molecules. Thus, persistent circulation of these NPs can be promoted (50).

Up to now, few attempts have been made to apply solid inorganic nanoparticles as a vaccine delivery platform. Iron oxide nanoparticles (IONs) are one kind of solid inorganic nanoparticles. They are suitable for many biomedical applications due to their good biocompatibility, magnetic characteristics, the availability for multiple surface functionalization, and low cost (51; 52). They have been applied in optical imaging and magnetic targeting in tumors (53), targeting primary breast cancers and metastases (54), and delivery of antibodies against breast cancer (55).

IONs have safety profiles, prior uses in drug delivery, and low cost of production. Surface modification makes it available to conjugate with proteins, peptides and DNA (56). Therefore, it

is a potential delivery platform for vaccines. Considering peptides are generally not very immunogenic on their own and require additional components to stimulate an adequate response (57), IONs may function as adjuvants to stabilize antigens and increase cellular uptake, trafficking and presentation of the antigens. George Hui, *et.al* first demonstrated that iron oxide nanoparticles could be applied as a clinically acceptable vaccine delivery platform without additional adjuvants (58).

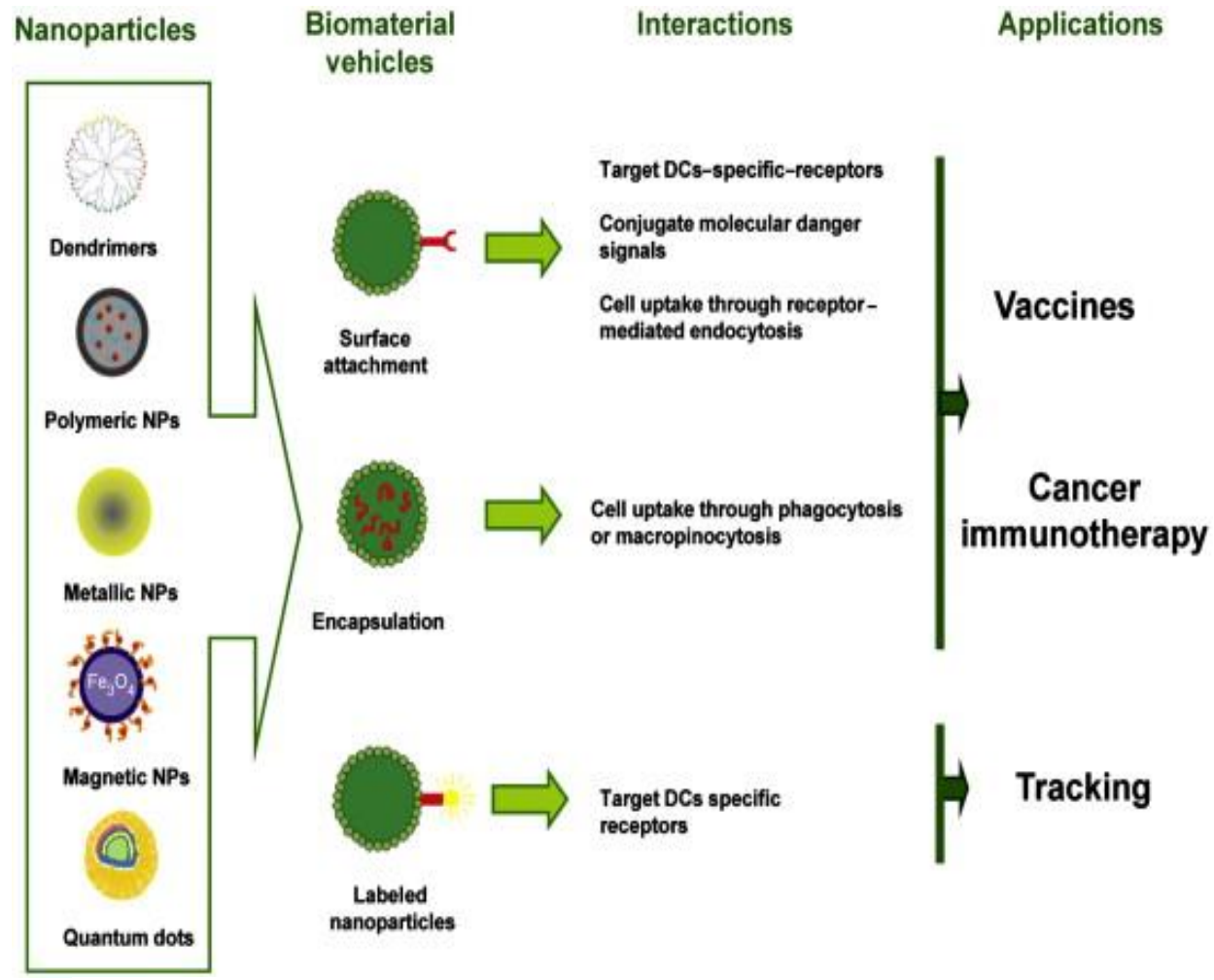

Fig. 1.4. Different strategies of nanoparticle (NPs) targeting. Figure is adapted from (41).

1.3.3 ION as delivery platform of influenza vaccine

We hypothesized that the ION could display as a delivery platform for influenza vaccine and present the peptides to DCs and elicit subsequent adaptive immune response without additional adjuvants. In order to testify this hypothesis, we developed a HA subunit influenza vaccine delivered by ION in this study. The recombinant HAs (HA without the transmembrane polypeptide and cytoplasmic domain) from influenza A virus A/Vietnam/1203/04 (H5N1) was sub-cloned into an *E.coli* expression system. After confirming the correct expression of HAs in bacterial cultures, we purified and refolded the recombinant HA proteins. Furthermore, the immunogenicity of the noval nano-vaccine was characterized in Balb/c mice. The mice were immunized with different doses of HAs with the addition of IONs or commercial adjuvants to investigate the anti-HA antibody responses elicited in the immunized mice. Therefore, we explored the immunogenicity of the recombinant HAs and compared the adjuvant effects of IONs and the commercial adjuvants.

II. MATERIALS AND METHODS

2.1. Plasmid constructs

2.1.1. Expression system

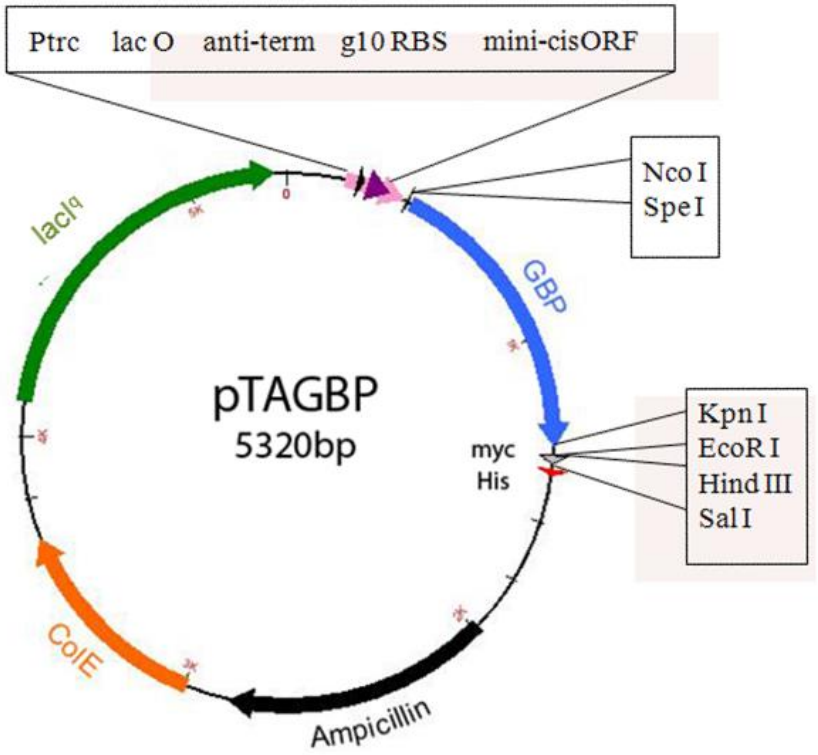

Fig. 2.1. A plasmid map of the pTAGBP vector.

pTAGBP, an established expression vector from Dr.Ye's lab (shown in Fig. 2.1.), was constructed from pTrcHis2-TOPO (Invitrogen Corporation,Carlsbad, CA). The DNA sequence of HA protein was amplified from pCDNA3.01/HA/optimized provided by Dr.Gao (26).

The pTAGBP vector has important elements as listed below:

- The trc promoter is a hybrid promoter containing the –35 region from the trpB promoter and the –10 region from the lacUV5 promoter. This hybrid promoter works sucessfully for high-level expression in *E. coli*.

- The lacO sequence is an important operator in this expression system. It is the binding site of the Lac repressor encoded by *lacI*^{q} gene. In the absence of IPTG, Lac repressor binds to the lacO sequence and represses transcription. The binding between IPTG and Lac repressor results in the deattachment of Lac repressor from the LacO sequence so that the expression is induced.
- rrnB antitermination sequence functions to reduce premature transcription termination.
- T7 gene 10 translational enhancer sequence strenghtens the translational initiation.
- The minicistron containing nucleotides that are efficiently translated in prokaryotic cells is included in this vector to enhance translational efficiency.
- The C-terminal 6xHis tag serves for purification of the recombinant proteins.

2.1.2. Plasmid extraction

E.coli was grown in Luria-Bertani media (LB broth, 1.0% Tryptone, 0.5% yeast extract, 1.0% NaCl, pH 7.0, Thermo Fisher Scientific Inc., Rockford, IL) supplemented with 0.4% Glucose and 100 µg/ml Ampicillin when necessary. To extract the plasmids, a portion of 10 µl *E.coli* glycerol stock (kept at -80ºC) of pCDNA3.01/HA/optimized was added into 5 ml LB media and incubated at 37 ºC with a speed of 250 rpm overnight. The plamids were extracted using PureYield™ plasmid miniprep kit (Promega Corporation, Madison, WI): a portion of 3 ml overnight bacteria culture was collected by centrifuging in a microcentrifuge for 30 s at 13,000 rpm, and the supernatant was discarded. The pellets were resuspended in 600 µl deionized water (dH_2O). To prepare the lysate, 100 µl of Cell Lysis Buffer (Blue) was added into the mixture and the tubes were inverted 6 times. After that, 350 µl of cold (4–8°C) Neutralization Solution was added into the mixture and mixed thoroughly by gently inverting. The debris after lysis was removed by centrifuging at 13,000 rpm in a microcentrifuge for 3 min. Without disturbing the

cell debris pellet, the supernatant containing the DNA (~900 µl) was transferred to a PureYield™ Minicolumn and centrifuged at 13,000 rpm for 15 s. The flowthrough was removed, and the minicolumn, with the DNA bound to its matrix, was put back into the same collection tube. To wash the minicolumn, 200 µl of Endotoxin Removal Wash (ERB) was added to the minicolumn and centrifuged at 13,000 rpm for 15 s. A volume of 400 µl Column Wash Solution (CWC) was added to the minicolumn followed by centrifuging at 13,000 rpm for 30 s. Before eluting the plasmid DNA, the minicolumn was transferred to a clean 1.5 ml microcentrifuge tube, then 30 µl of nuclease-free water was added directly to the minicolumn matrix. After standing for 1 minute at room temperature (RT), the plasmid DNA was eluted by centrifuging for 15 s. A volume of 2 µl eluted plasmid DNA was dropped onto Take3 plate to measure its concentration. The rest was stored at –20°C for further use.

2.1.3. Polymerase Chain Reaction (PCR)

The cytoplasmic and transmembrane domain sequences of the HA were removed from the HA gene during PCR amplification and the truncated HA gene was referred as HAs. The pCDNA3.01/HA/optimized plasmid extracted from *E.coli* was used as a template for PCR. The Spe I and Sal I restricted sites in the pTAGBP vector were selected for subcloning of HAs. For construction of the HA expression vector, the following set of PCR primers was used: **HAs (forward)** (5'-ATAGACTAGTGATCAGATCTGCATCGGT-3') and **HAs (reverse)** (5'-ACGCGTCGACATAGATGCCGATACTC-3'). The truncated HA gene was amplified by PCR with Phusion™ polymerase (New England Biolabs Inc., Ipswich, MA) in the presence of Phusion™ HF buffer (1.5 mM $MgCl_2$). The reaction system (50 µl) comprised of the following components: 5×Phusion™ HF buffer (10 µl), 10 mM dNTPs (1 µl), forward primer (1 µl), reverse primer (1 µl), template plasmid (1 µl, ~6ng), Phusion™ DNA polymerase (0.5 µl) and

deionized H_2O (dH_2O, 35.5 µl). Applied Biosystem 2720 Thermal Cycler was used to run the reaction. The PCR was carried out under the following conditions: initial denaturation at 98°C for 30 s, denaturation at 98°C for 10 s, annealing at 51°C for 30 s and extension at 72 °C for 48 s, repeated for 25 cycles and final extension of 72°C for 10 min.

After the PCR finished, a portion of 5 µl PCR product was mixed thoroughly with 1µl 6×DNA loading buffer (2.5% Ficolli-400, 11 mM EDTA, 3.3 mM Tris-HCl [pH 8.0], 0.017% SDS and 0.015% bromophenol blue, New England Biolabs Inc.) and analyzed by DNA electrophoresis in 0.8% agarose gel which contains 0.5 µg/ml ethidium bromide (EB). Quick-Load 1kb DNA ladder (New England Biolabs Inc.) was used as the marker. The gel was running in TAE (Tris-acetate-EDTA) buffer at 100 V for 40 min. The size of the PCR product was checked by a ultraviolet transilluminator. The positive products were purified using MinElute PCR Purification Kit (Qiagen Inc., Valencia, CA) by following a protocol provided by manufacturer.

2.1.4. Enzyme digestion

A portion of 1 µg of the HAs amplified sequence and the pTAGBP vector was double-digested in separate reactions using SalI-HF and SpeI (New England BioLabs Inc.). The other components of the digestion system include 10×buffer 4 (2 µl), SalI-HF (20,000U, 0.5 µl), SpeI (10,000U, 0.5 µl), 100× bovine serum albumin (BSA, 0.2 µl) and dH_2O to make the total volume of the reaction system 20 µl. The mixture was incubated at 37℃ for 1 h.

To check whether the HAs sequence and vector were correctly digested by the restriction enzymes, the products were mixed thoroughly with 4 µl 6×DNA Loading buffer and loaded onto 0.8% agarose gel which contains EB. The gel was running in TAE buffer at 100V for 40 min. After checking their sizes, the DNA bands were excised from the agarose gel and then purified

using gel extraction kit (Qiagen Inc.): three columes of Buffer QG was added to 1 volume of gel (100 mg~100 ul). The gel was dissolved by incubating at 50℃ for 10 min. Then one gel volume of isopropanol was added to the sample to increases the yield of DNA fragments <500 bp and >4 kb. To load DNA, the sample was applied to the QIAquick colume and centrifuged for 1 min at 13,000 rpm. The flowthrough was discarded and 0.75 ml of Buffer PE was added to wash the column and centrifuged for 1 min. After centruging for an additional 1 min, the QIAquick column was put into a clean 1.5 ml microcentrifuge tube. A volume of 50 ul dH_2O was added to the center of the QIAquick membrane to elute the DNA. After standing for 1 min, the column was centrifuged for 1 min. The purified DNA was stored at -20 ℃.

2.1.5. Ligation

T4 DNA Ligase Kit (Thermo Fisher Scientific Inc.) was applied to join the restriction enzyme generated DNA fragments. This enzyme catalyzes the formation of a phosphodiester bond between juxtaposed 5'-phosphate and 3'-hydroxyl termini in duplex DNA. The insert DNA was 5:1 molar ratio over vector. The components of the reaction included 10×T4 DNA Ligase Buffer (2 µl), vector (2 µl), HAs insertion (1.5 µl) and dH_2O (13.5 µl). The reaction occurred by incubating at 22℃ for 10 min. Thus, the HAs inserts were sub-cloned into pTA vector and the resultant expression plasmids were referred to as pTAHAs, as shown in Fig.2.2.

2.2. *E.coli* Transformation

2.2.1. *E.coli* strain

After the recombinant *E.coli* strain pTAHAs was completed, the vector was transferred into NEB 5- α competent *E. coli* [*fhuA2 Δ(argF-lacZ)U169 phoA glnV44 Φ80 Δ(lacZ)M15 gyrA96 recA1 relA1 endA1 thi-1 hsdR17*] (New England Biolabs Inc.). This DH5α^{TM} have several features to make it suitable for recombinant DNA sub-cloning:

- Δ*(lacZ)*M15 allows for blue/white screening for recombinant cells through α-complementation of the β-galactosidase gene.
- The recA1 mutation reduces homologous recombination and prevents the cloned plasmids from being alternated.
- The endA1 mutation incapacitates the activity of nonspecific endonuclease I to enhance the high quality plamid preparations.
- The hsdR17 mutation deactivates the restriction endonulease of EcoKI enzyme complex so that the unmethylated DNA from foreign plasmid can be efficiently transformed.

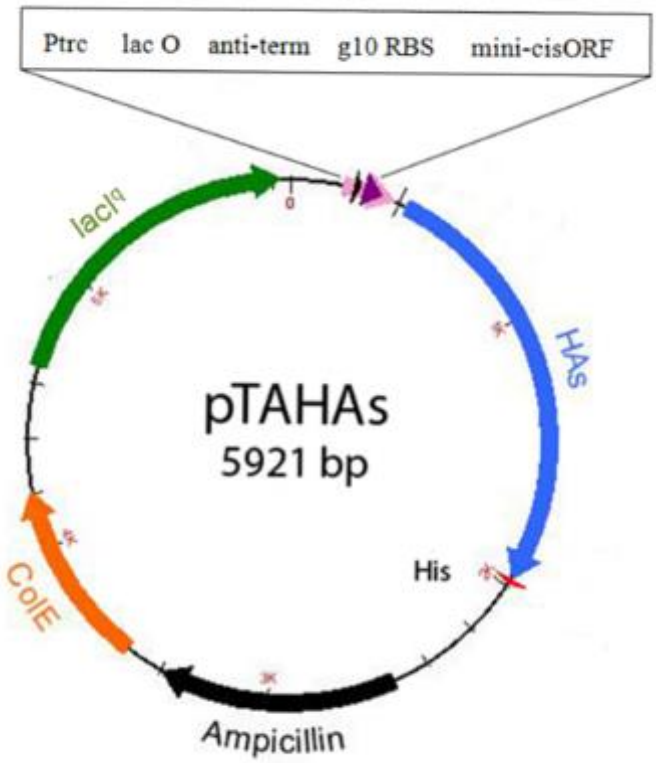

Fig. 2.2. Plasmid maps of pTAHAs expression vector.

2.2.2. Heat shock method

The competent cells are bacteria which can accept extra-chromosomal DNA or plasmid. The commercial competent cells can uptake the ligated recombinant plasmids by heat shock method. The competent cells were thawed on ice for 10 min in advance. When the ligation finished, 7 μl ligation product was added into 25 μl DH5α competent cells and the mixture were put on ice for 30 min, followed by heating at 42 °C for 30 s. After incubating for another 5 min on ice, the mixture was added into 475 μl SOC media (0.5% Yeast extract, 2% Tryptone , 10 mM NaCl, 2.5 mM KCl, 10 mM $MgCl_2$, 10 mM $MgSO_4$, 4% glucose) provided along with the competent cells by New England Biolabs Inc. and shaked at 37°C for 1 h with a vigorous shaking at 150 rpm in an incubator shaker. A volume of 50 μl or 100 μl of cells were spread onto LB selection plates (1.0% Tryptone, 0.5% yeast extract, 1.0% NaCl, 1.5 % agar) containing 100 μg/ml Ampicillin and incubated overnight at 37℃.

2.2.3. Verification of transformed plasmids

To confirm the correct insertion, five colonies were picked up from each plate and inoculated in 5 ml LB media containing 100 μg/ml Ampicillin overnight at 37°C with shaking at 250 rpm overnight. The plasmids of the recombinant *E.coli* were extracted using the same methods described in 2.1.3. After that, the plasmid were digested by the same restriction enzymes as described in 2.1.5. The size of the digested fragments were checked by DNA electrophesis (0.8 % agarose gel containing EB).

Because mutations might happen during the cloning process, we need to further confirm the correction of the insertion via DNA sequencing. Samples which included 3.4 pmol primers, 300-500 ng plasmid and dH_2O with the total volume of 13 μl, were submitted to the UA DNA Resource Center for capillary sequencing. After confirming that the sequence of the colonies

were correct, 400 µl culure of each confirmed *E.coli* strains were mixed thoroughly with 100 µl 100% glycerol and stored at -80℃.

2.3. Expression of HAs proteins in *E.coli*

2.3.1. Induction of the recombinant proteins

To induce the expression of recombinant proteins in *E.coli*, a volume of 10 µl cell culture from storage tube was inoculated in 5 ml LB media (supplemented with 0.4% glucose and 100 µg/ml Ampicillin) and grown overnight at 37°C with shaking at 250 rpm overnight. The next day, a portion of 0.5 ml overnight culture was inoculated in 50 ml LB media with vigorous shaking. A volume of 1 ml sample was taken 16 h post cultivation to determine the cell density by measuring OD_{600} using a spectrophotometer. When the OD_{600} reached 0.6 which indicated that the cells were in mid-log phase, volume of cells equivalent to 1 OD_{600} was removed and centrifuged at 5,000 rpm for 10 min. The supernatant was aspirated and the cell pellet was frozen at -20°C as sample of 0 h.

The inducer IPTG was added to the culture to a final concentration of 1mM. The culture was kept incubation at 37°C with shaking at 250 rpm. To determine the optimal induction time point, volume of cells equivalent to 1 OD_{600} was removed every hour for 8 h and treated as described above.

2.3.2. Separation of soluble and insoluble expressed proteins

The recombinant proteins expressed in bacteria usually form inclusion bodies when they are expressed at high levels. These inclusion bodies can be separated from bacterial cytoplasmic proteins easily by centrifugation. B-PER II bacterial protein extraction reagent (Pierce Biotechnology, Rockford, IL) was applied to effectively extract soluble proteins.

Frozen pellet bacterial cells were washed once with 1× PBS buffer (137 mM NaCl, 2.7 mM KCl, 10 mM Na_2HPO_4, and 1.8 mM KH_2PO_4, pH 7.4) by centrifugation at 13,000 rpm for 5 min at 4°C. For Mini-Scale Bacterial Protein Extraction (1.5 ml bacterial culture, OD_{600} = 1.5-3.0), washed cells were re-suspended in 150 µl B-PER II reagent by vigorously vortexing until the cell suspension was homogeneous. After vortexing for additional 1 min, soluble proteins were separated from insoluble proteins by centrifugation at 13,000 rpm for 5 min at 4°C. For Midi-Scale Bacterial Protein Extraction (40 ml bacterial culture, OD_{600} = 1.5-3.0), washed cells were re-suspended in 2.5 ml B-PER II reagent by vigorously vortexing until the cell suspension was homogeneous. After the mixture was shaken gently at RT for 30 min, soluble proteins were separated from the insoluble proteins by centrifugation at 13,000 rpm for 15 min at 4°C.

The supernatant (soluble fraction) was collected and the pellet (insoluble fraction) was re-suspended in same volume of B-PER II that used to extract the proteins. A volume of 20 µl fraction was mixed with 4 µl 6×loading buffer (375 mM Tris-HCl pH 6.8, 12% SDS, 30% glycerol, 600 mM DTT, and 0.12% bromophenol blue) for SDS-PAGE (Sodium dodecyl sulfate polyacrylamide gel electrophoresis) or Western blotting assay to determine the solubility of the recombinant protein.

2.3.3. SDS-PAGE and western blotting

The soluble and insoluble fractions from samples equivalent to 1 OD_{600}, which were collected at different time points, were heated at 95 °C for 5 min. The sample was mixed before and after the heating step by vortexing. After the samples cooled to RT, debris were removed by centrifuging at 15,000 rpm for 10 min. Polyacrylamide Tris-glycine gels (10%) were prepared using the components in Table 2.1. A portion of 15 µl supernatant was loaded per well onto the

gel with special gel loading tips, and 7 µl of Precision Plus Protein WesternC Standards (Bio-Rad Laboratories, Inc., Hercules, CA) was loaded in separated well alongside the samples.

10% Separating Gel	1 gel	2 gel	5% Stacking Gel	1 gel	2 gel
dH_2O	1.9 ml	4.0 ml	dH_2O	1.4 ml	2.7 ml
1.5 M Tris (pH 8.8)	1.3 ml	2.5 ml	1.0 M Tris (pH 6.8)	250 µl	500 µl
30% Acrylamide	1.7 ml	3.3 ml	30% Acrylamide	330 µl	670 µl
10% SDS	50 µl	100 µl	10% SDS	20 µl	40 µl
10% APS	50 µl	100 µl	10% APS	20 µl	40 µl
TEMED	2 µl	4 µl	TEMED	2 µl	4 µl

Table 2.1.Components of SDS-PAGE gel (0.75 mm)

Electrophoresis was performed in the TGS running buffer (25 mM Tris, 192 mM glycine, 0.1% SDS, pH 8.3) at 100 V for 30 min (stacking gel) and then at 200 V for 1 h (separation gel). After electrophoresis, the gel was carefully removed from the cassette.

For protein staining, the gel was immerged into staining buffer (0.25% Coomassie Brilliant Blue R-250 Staining solutions (Bio-Rad), 40% methanol, 10% acetic acid) for 1 h at RT with gentle mixing on a rotary shaker. To visualize the protein, the gel was then destained by destaining buffer (30% methanol, 10% acetic acid) at RT until the gel became transparent.

For Western blotting, the proteins on the gel were transferred to nitrocellulose membrane. Fresh transfer buffer (25 mM Tris, 192 mM Glycine, 0.1% SDS, 20% methanol, pH 8.3) was prepared and cooled at -20°C. A sheet of nitrocellulose membrane with the pore size of 0.45 µm (Bio-Rad Laboratories, Inc.) was cut to appropriate size. The membrane, the gel, filter papers (Bio-Rad Laboratories, Inc.) and sponges were pre-wet in transfer buffer and kept in 4°C for 10 min. A “sandwich” blot assembly was packed as: sponge-filter paper-gel-nitrocellulose

membrane-filter paper-sponge. All the bubbles in between were carefully removed by pipette during packing. The "sandwich" assembly was located in an ice tray which was placed in a box filled with cooled transfer buffer. Thus, the proteins on SDS-PAGE gel were transferred to 0.45 μm nitrocellulose membrane in a constant voltage of 150 V for 50 min. After transferring, the membrane was carefully removed from the cassette using tweezers and incubated in a blocking buffer (1×PBS, 0.05% Tween-20, 5% non-fat dry milk) for 2 h with shaking at RT. After blocking, the membrane was incubated in mouse anti-HA antibody (BEI resource, Manassas, VA) diluted in non-fat dry milk/PBST (1×PBS, 0.05% Tween-20, 1% non-fat dry milk) at a ratio of 1: 500 (v/v) at 4ºC with shaking overnight. The membrane was then washed with PBST (1×PBS, 0.05% Tween-20) three times, 5 min each time, and incubated with anti-mouse IgG horse peroxidase (HRP) conjugated antibody (Sigma-Aldrich, St. Louis, MO) diluted at a ratio of 1: 2,000 (v/v) in non-fat dry milk/PBST. After shaking at RT for 1 h, the membrane was washed three times with PBST, 5 min each, followed by PBS, one time. Subsequently, the enhancer and stable peroxidase solutions (Thermo Fisher Scientific Inc.) were 1:1 (v/v) mixed and carefully loaded onto the membrane and incubated in dark for 5 min. The membrane was imaged using Molecular Imager ChemiDoc XRS System (Bio-Rad Laboratories, Inc.) and analyzed using PDQuest Analysis software (Bio-Rad Laboratories, Inc.).

2.4. Purification of HAs proteins

2.4.1. Solubilization of the denatured proteins

A large volume of 400-500 ml culture was incubated and induced as described in 2.3.1. A portion of 0.75 ml buffer B (100 mM NaH_2PO_4, 10 mM Tris-HCl, 8 M urea, pH 8.0) was added to the pellets collected from every 50 ml culture (3.5 h post induction). In order to solubilize the proteins inside the inclusion bodies, the pellets were re-suspended and shaken at RT for 2 h. The

supernatant was collected by centrifugation at 14,000 rpm for 20 min at 4 °C. Syringe filters with the pore size of 0.45 µm (EMD Millipore, Billerica, MA) were applied to filter the solubilized protein sample and all the buffers before use in the purification.

2.4.2. Purification of HAs using NTA-Ni resin under denaturing conditions

The Ni-NTA superflow slurry (Qiagen Inc.) was resuspended and poured into the column until 1ml resin was settled. After that, the column was equilibrated with 5ml volumes of buffer B. Wash buffer C and elute buffer D were prepared with the same components but with pH 6.3 and pH 5.0, separately. A_{280} was measured by spectrophotometer to indicate the existence of proteins in solution. The sample was applied to column at a speed of 0.2 ml/min and washed with buffer B at a speed of 1 ml/min until the A_{280} is below 0.01. The column was then washed with buffer C until the A_{280} is below 0.01. Protein was finally eluted with buffer D with the speed of 0.2 ml/min, collected by 1 ml/tube. A volume of 20 µl of flow-through, wash fraction and each elute fraction were collected for SDS-PAGE assay.

2.4.3. Dialysis and concentration of proteins

The eluted proteins were refolded by removing the urea through dialysis. Float-A-Lyzer G2-20K (Spectrum Laboratories, Inc., Rancho Dominguez, CA) dialysis tubes were soaked in 10% ethanol followed by thoroughly flushing and soaking in dH_2O before use. The sample was then loaded to the tube and refolded by stepwise dialysis against buffer 1 (6 M urea, 0.5 M NaCl, 1 mM DTT) at 4°C for 6 h. Buffer 1 was diluted against buffer 2 (25 mM Tris-HCl, pH 7.5, and 150 mM NaCl, 1 mM DTT,

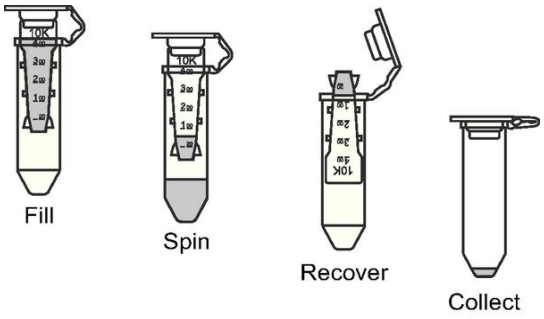

Fig. 2.3. Usage of the Amicon Ultra concentration tube. Figure is adapted from product manual.

0.1 mM EDTA). Sample was then dialyzed against 4M urea buffer for 6 h and against 2 M urea buffer for 8 h. Finally, proteins were dialyzed against buffer 3 (25 mM Tris-HCl, pH 7.5, 0.9% NaCl) for another 4 h.

Amicon Ultra-0.5 (EMD Millipore) was applied to concentrate the dialyzed HAs proteins. The centrifugal filters with a pore size of 10kDa allow protein no larger than 30 kDa go through the membrane, so that the HAs protein (58.7 kDa) will remain in the inner collection tubes. As shown in Fig. 2.3., up to 0.5 ml sample was added to the Amicon Ultra filter device, followed by spinning at 14,000 g for 15 min. The concentrated solute was then recovered by placing the filter device upside down in a clean micro centrifuge tube and spun at 1,000 g for another 2 min.

2.4.4. BCA Assay

For quantification of the recovered proteins after dialysis, the concentration of proteins was detected by BCA Protein Assay kit (Pierce Biotechnology) using microplate procedure. Stock of BSA was 2-folded diluted from 2,000 μg/ml to125 μg/ml. A portion of 25 μl diluted BSA standard and dialyzed protein sample was added into wells of 96 well plate. The working reagent (WR) was prepared by mixing 50 parts of BCA Reagent A with 1 part of BCA Reagent B (50:1, Reagent A: B). A portion of 200 μl WR were added to each well. After mixing the samples and WR, the plate was covered and incubated at 37°C for 30 min. The absorbance was measured at 562 nm using a microplate reader (BIO-TEK, Winooski, VT) when the plate cooled to RT.

2.5. Animal studies

2.5.1. Mice

Female Balb/c mice at seven weeks of age, purchased from the Jackson Laboratory (Bar Harbor, ME), were used in all animal experiments described in this study. Mice were kept in a pathogen-free Biosafety level-2 animal facility in the Central Laboratory Animal Facility (CLAF) at

University of Arkansas (Fayetteville, AR). All procedures were conducted according to Institutional Animal Care and Usage Committee (IACUC) approved protocol #13056. Five mice were raised in each cage and they were labeled by 0-2 cuts on their left or right ear as: blank (B), left-1 (L-1), left-2 (L-2), right-1 (R-1) and right-2 (R-2).

2.5.2. Vaccine preparation

The iron oxide nanoparticles (IONs) coating with NTA-Ni (SHT) or with COOH (SHP) were prepared by the Ocean Nanotech LLC and kept at 4°C during delivery. For conjugation, SHT particle was mixed with HAs protein (~200 μg/ml) on a rotary shaker at 4 °C for 2 h (n ION: n Protein=1:5 as suggested by the company); SHP was mixed with HAs protein as negative control. A portion of 20 μl of the ION-HAs mixture was loaded to each well of 1% agarose gel to confirm that proteins are bound to the particle. For preparation of the nano-vaccines, larger amount of HAs were bound to SHT using method as described above. Unbounded HAs proteins were removed by centrifugal filter (100 kDa, EMD Millipore), centrifuging at 14,000 rpm for 20 min at 4 °C. Their concentration (in the filtration liquid) was measured by BCA assay (described in 2.4.4) so that the loading efficiency of HAs could be calculated. The other kind of nano-vaccines were prepared by mixing HAs with SHP without specific binding. For all the groups (n=3), mice were injected with the same volume (50 μl). Nano-vaccines for injection of mice in the same group were prepared in one 1.5 ml tube and buffer 3 in the dialysis step was used to adjust the total volume. Because there was space in the needle hub, nano-vaccine with a total volume of 300 μl (doses for 6 mice) was prepared for each group.

2.5.3. Immunization

In the preliminary experiment, SHT-HAs nano-vaccines carrying 2 μg or 4 μg recombinant HAs proteins were investigated. Groups of seven-week-old female Balb/c mice (n=3) were used in

order to provide statistically meaningful data. The nano-vaccines were injected into mice via intramuscular route (i.m.). Complete Freund's adjuvant (CFA) is a water-in-oil emulsion containing killed cells of *Mycobacterium butyricum* and used in initial injections, while incomplete Freund's adjuvant (IFA), which lacks this bacterium, is used for subsequent injections. Control mice were immunized with 2 μg HAs emulsified 1:1 (v/v) with CFA/IFA (Thermo Scientific, Rockford, IL), saline only or SHT only, respectively. Syringes (1 ml) with Luer-Loc tip and 26 G×1/2 in. needles from Becton Dickinson (Franklin Lakes, NJ) were applied for injection of the HAs emulsified with CFA/IFA, whereas syringes (1ml) with tuberculin slip tip and 30 G×1/2 in. needles were used for the rest groups (shown in Fig. 2.4[A]). The area to be injected was first swabbed by 70% ethanol to let the skin expose, the tip of the needle was then inserted through the skin and into the caudal thigh muscles (Fig. 2.4[B]). In all cases, the mice were injected three times (two weeks between each injection). The weight of each mice was recorded and the activity of mice was observed every another day since the prime immunization.

With experienced manipulation, nano-vaccines carrying 6 μg or 8 μg recombinant HAs proteins were investigated. In this experiment, we tested two kinds of IONs: SHT (binding with HAs via the chelation of NTA-Ni) and SHP (mixing with HAs without specific binding). Control mice were immunized with 6 μg HAs emulsified with CFA/ IFA, 6μg HAs only, saline only or SHT only, respectively. Still, the mice were injected three times (two weeks between each injection) and the weight and activity of each mouse was recorded every another day since the prime immunization. Details of mice immunization are listed in Table 2.2.

2.5.4. Bleeding

To determine the humoral immune responses in the immunized mice by serological evaluation of the production of anti-HA immunoglobulin, approximately 100 µl of blood samples were taken on day 10, 24 and 38 post-immunization from submandibular vein. As shown in Fig. 2.4 (C),

Group	Vaccine	Dose (µg/50µl)	#Mice
1	SHT-HAs*	2	3
2	SHT-HAs*	4	3
3	HAs+CFA/IFA	2	3
4	SHT*	0	3
5	Saline	0	3
Group	**Vaccine**	**Dose (µg/50µl)**	**#Mice**
1	SHT-HAs*	6	3
2	SHT-HAs*	8	3
3	SHP+HAs*	6	3
4	SHP+HAs*	8	3
5	HAs+CFA/IFA	6	3
6	HAs	6	3
7	SHT*	0	3
8	Saline	0	3

Table 2.2. Experimental mice grouping (vaccination through i.m. route)

***** It has been demonstrated that up to 4.4 mg/injection of IONs does not cause any abnormalities or changes in the blood chemistry of mice tested after each of the three immunizations (58) and that the total dose of the ION-HAs vaccines, of which the IONs are only a fraction, will be well below this amount.

goldenrod animal lancets with 4 mm of point length (MEDpoint, Inc., Mineola, NY) were applied to collect the blood sample. Detailed procedures for this blood sampling are described elsewhere (http://www.medipoint.com/html/directions_for_use1.html). This bleeding procedure causes only momentary pain and distress. The 1.5 ml tubes those contained the collected blood samples stood at RT for 3 h and was then centrifuged at 2,500 rpm for 10 min. The supernatant (serum containing anti-HA antibody) was transferred to PCR tubes and kept at -20°C.

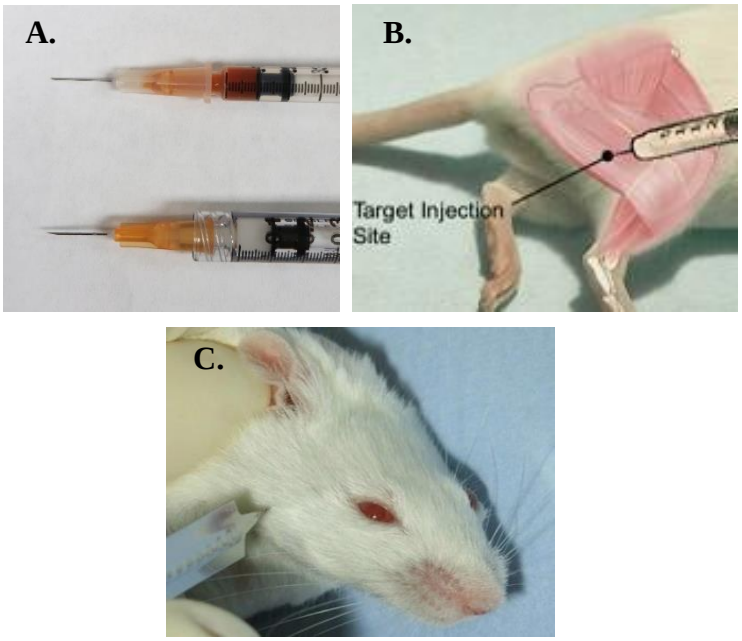

Fig. 2.4. A. Syringes and needles used in mice immunization. Upper: SHT conjugated with HAs; Below: HAs emulsified with CFA (Photo taken by the author of the thesis); **B. The site of intramuscular injection of mice** (adapted from http://www.theodora.com/rodent_laboratory/injections.html); **C. Bleeding from submandibular vein** (adapted from www.medipoint.com).

2.5.5. Enzyme-linked Immunosorbent Assays (ELISA)

Costar Flat Bottom High-binding 96-well EIA/RIA plates (Fisher Scientific) were coated with HA proteins (2 μg/ml) of influenza virus A/Vietnam/1203/2004 (H5N1) from BEI resources. The HA proteins were dissolved in coating buffer (0.16% Na_2CO_3, 0.292% $NaHCO_3$, 0.016% NaN_3, pH 9.6, filtered with 0.2μl filter). A portion of 100 μl of HA proteins per well was added to the 96 well plates and incubated overnight at 4°C. The next day, the coating buffer was removed and plates were washed twice by TBST (20 mM Tris-base, 150 nM NaCl, 0.05% Tween-20, pH 7.3). A portion of 200 μl blocking buffer (20 mM Tris-base, 150 nM NaCl, pH 7.3, 0.05% Tween-20, 1% BSA) was then added to each well. After 2 h blocking at RT, plates were washed with TBST four times. After that, thawed mouse sera were 2-fold sequentially diluted in the blocking buffer. A volume of 100 μl of these 2-fold sequentially diluted sera was added to each well and incubated for 2 h at 37°C. Plates were then washed with TBST four times. Afterwards a portion of 100 μl of 5,000 diluted Goat anti-mouse IgG Biotinylated Affinity (R&D, Fisher Scientific) in blocking buffer was added to each well and incubated for 1h at 37°C. Plates were then washed by TBST four times. A portion of 100 μl of 1,000 diluted Streptavidin-Alkaline Phosphatase (R&D, Fisher Scientific) in blocking buffer was added to each well and incubated for 1 h at 37°C. Plates were then washed by TBST five times. A volume of 100 μl p-Nitrophenyl Phosphate Liquid Substrate (MP Biomedicals, Fisher Scientific) was added to each well and incubated in dark for 25 min. The reaction was stopped by addition of 50 μl of 2 M NaOH to each well and the color intensity was measured immediately at 405 nm and 630 nm with a microplate reader (BIO-TEK). Sera collected from mice injected with saline served as negative control.

Serum samples were 2-fold diluted from 2^{-3}-2^{-8} dilution. Further dilutions were performed if necessary. The endpoint titer was defined as the reciprocal of the serial serum dilution at which

the (OD_{405nm}-OD_{630nm}) was above 0.2, which was also larger than the mean plus three standard deviations (CN+ 3SD) of the value of the negative control samples. Values of p for differences between mean titer of the diversely immunized animal groups were determined by paired Student t-test using Excel. A 95% confidence interval will be applied to determine the statistical significance of differences between groups.

III. RESULTS AND DISCUSSION

3.1. Construction of pTAHAs plasmid

To construct the pTAHAs plasmid, we inserted the HAs gene fragment into a pTAGBP vector and replaced the GBP gene with HAs. The HAs fragment (HA without cytoplasmic and transmembrane domain sequences) was amplified by PCR, as described in 2.1.3. After the reaction, a portion of 5 μl PCR product was removed for electrophoresis. A bright band was detected, as shown in Fig. 3.1., which indicated the HAs sequence of correct size (1562 bp) was amplified.

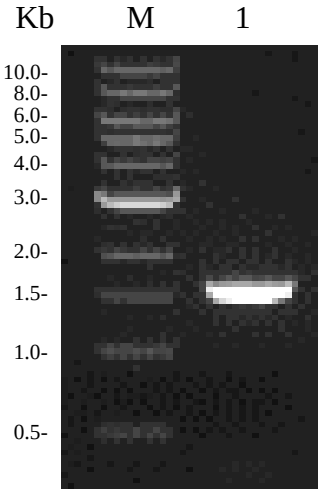

Fig. 3.1. PCR products of amplified HAs fragments using designed primers. Lane M, 1Kb DNA ladder; Lane 1, the PCR product. The samples were analyzed using 0.8% agarose gel.

The PCR products as well as the pTA vector was followed being digested by SalI-HF and SpeI double enzyme, both of the products were taken to run the agarose gel electrophoresis. The sizes of the bands were check under UV light. Showing correct sizes, these bands were cut off from the gel shortly after they were exposed to UV light. After purification, the digeste vector and insertion were ligated by T4 DNA Ligase and followed by heat shock transformation into competent *E. coli* cells.

The second day after the overnight incubation, two colonies were picked up from the LB plate with selective antibodies by loop. The plasmids of the selected colonies were extracted and screened for positive clones using restriction enzyme digeation assay as mentioned above. As shown in Fig. 3.2., two bands indicated the HAs was corrected inserted into the vecter. The larger band was between 4,000 bp and 5,000 bp, which was close to the size of the original backbone (4308 bp) and the small band was of a size similar to that of HAs (1562 bp).

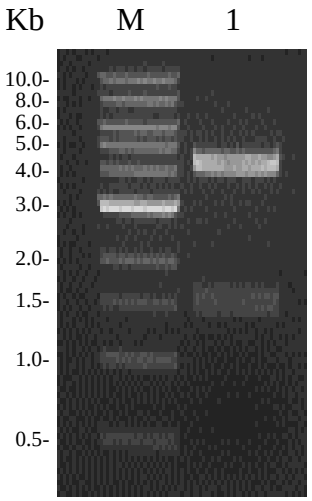

Fig. 3.2. Validation of recombinant DNA isolation through enzyme digestion. Lane M, 1 kb DNA marker; Lane 1, plasmid extracted from selected colony pTAHAs#1. The plasmid was digested with Spe I-HF and Sal I restriction enzymes and analyzed through electrophoresis using 0.8% agarose gel.

Afterwards, DNA sequencing confirmed that there was there was no point mutation in the positive colony identified through the enzyme digestion assay. The resultant plasmid was referred as pTAHAs (Fig.2.2.).

3.2. Detection of the expression of HAs in *E.coli*

The expression of HAs is induced by the addition of IPTG. The latter binds with *lac* repressor and releases them from the *lac* operator so that the transcription of HAs initiated. As the bacteria growth entered an exponential growth phase (OD_{600nm} reached 0.6), we added IPTG into the

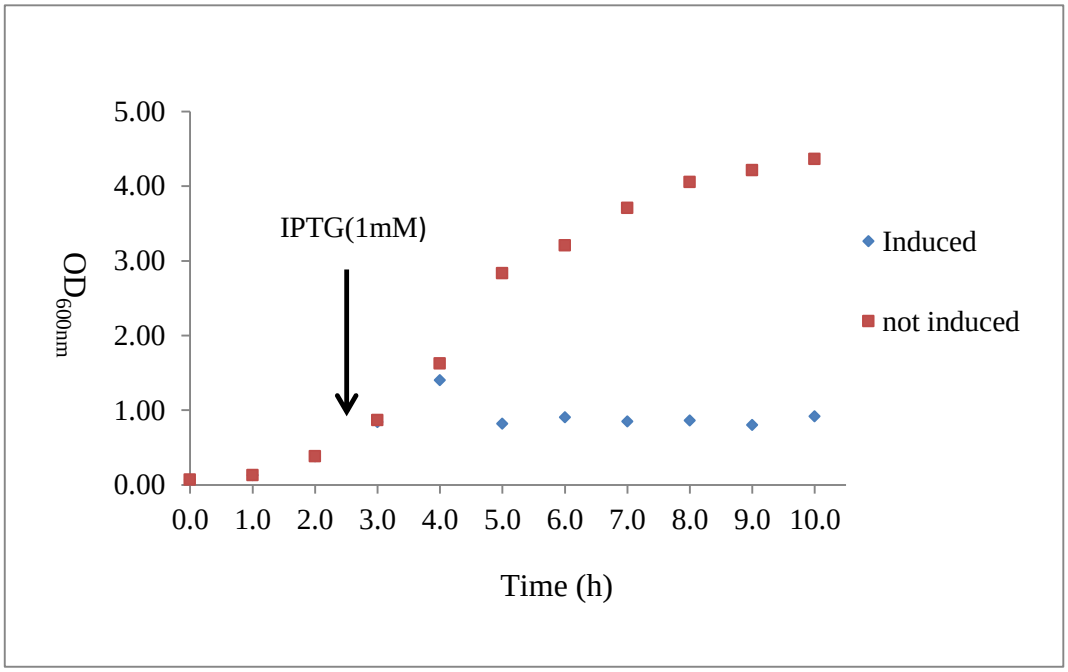

Fig. 3.3.The growth curve of E.coli DH5α harboring pTAHAs plasmid. Cells were grown in LB medium containing 0.4% glucose and 100µg/ml Ampicillin. IPTG was added to a final concentration of 1 mM at 2.5 h when OD_{600}nm approach 0.6. The *E.coli* growth was observed over 10 h culture period.

culture to a final concentration of 1mM in order to induce the expression of HAs. 1 ml culture was collected over a 10-h time period, with 1-h interval as mentioned in 2.3.1. The concentration of cells were measured as the absorbance at 600nm. The growths of induced and non-induced bacterial were compared (Fig. 3.3.). The bacterial without induction kept growing to an OD above 4 at 10 h, while the one with induction stopped growing since 4 h and their OD was maintained below 1. The obvious difference of growth speed also indicated that the expression of HAs protein brought growth pressure to the bacterial cells.

Next, we determined the solubility of the expressed HAs proteins and the optical induction time to gain highest expression level through SDS-PAGE assay. The samples collected as described above were treated by B-PER II bacterial protein extraction reagent as mentioned in 2.3.2., and the soluble proteins expressed by *E.coli* cells located in the supernatant after this step. Same

amount of extraction reagent was added to the pellet, and the latter as well as the supernatant were mixed with loading buffer and heated. In this way, the insoluble proteins were released from the inclusion bodies.

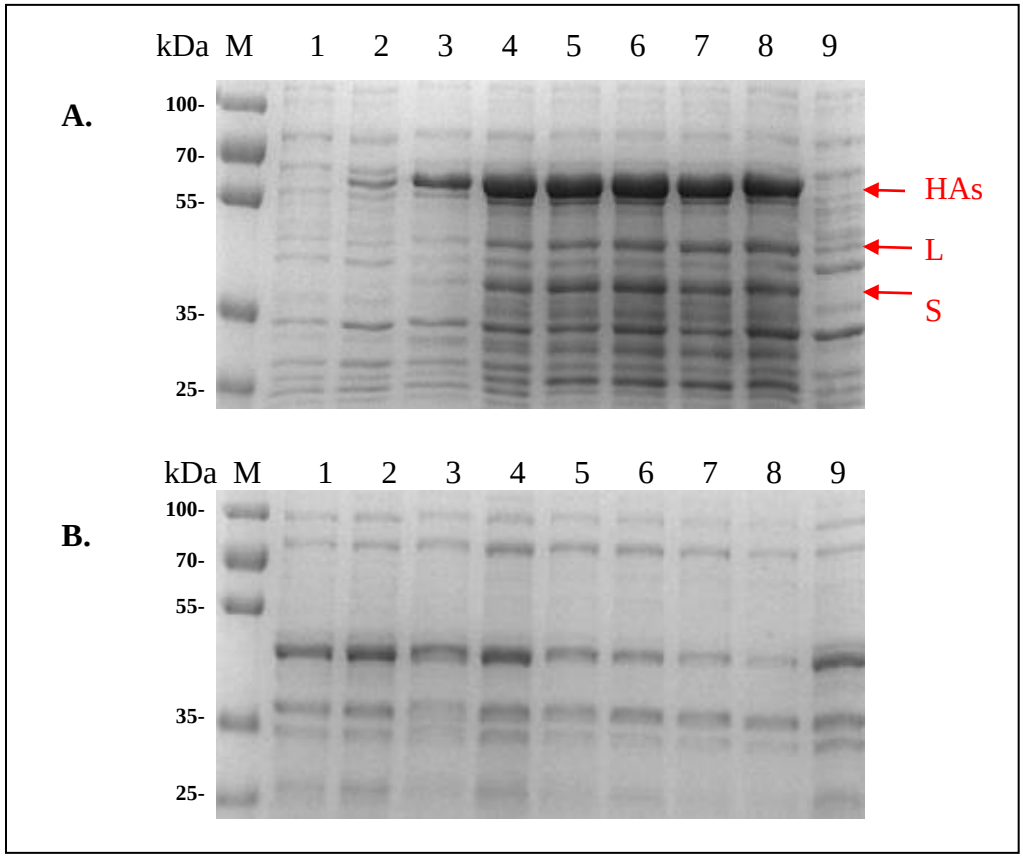

Fig. 3.4. Determination of optimal induction period of HAs expression in recombinant DH5α/pTAHAs by SDS-PAGE assay. A) Pellet (insoluble fraction); B) supernatant (soluble fraction); Lane: M, Protein ladder; 1, recombinant DH5α/pTAHAs before induction; 2-8, 0.5-6.5 h post induction; 9, recombinant DH5α/pTAHAs without induction 3.5 h after IPTG was added to the other culture. The proteins were separated by 10% SDS-PAGE gel.

The strong bands at position of 58.7 kDa in Fig. 3.4 (A) indicated that the HAs was expressed in *E.coli* cells. For there was no apparent bands in Fig. 3.4 (B), the expressed HAs were insoluble and located in inclusion bodies. It is noted that in Fig. 3.4 (A) the density of two bands between 35 kDa and 55 kDa was also increased. The larger band (L) showed in the sample before

induction (Lane 1), the non-induced sample (Lane 9), so it is the bacteria' own protein. On the other hand, the smaller band (S) did not show at either Lane 1 or Lane 9. It is possible that degradation happened during this process. Because the expressed HAs carried a His-tag at its C-terminal, the extra bands could be further removed during His-tag specific purification method. From Fig. 3.4 (A), it seems that the HAs started to express as early as 0.5 h post induction, and the expression level reached the highest between 3.5-4.5 h post induction. Because the concentration of samples collected 3.5 h post induction had higher cell concentration (Fig. 3.3.), we chose 3.5 h as optical induction time in order to cover the largest yield of bacterial cells in the following experiments.

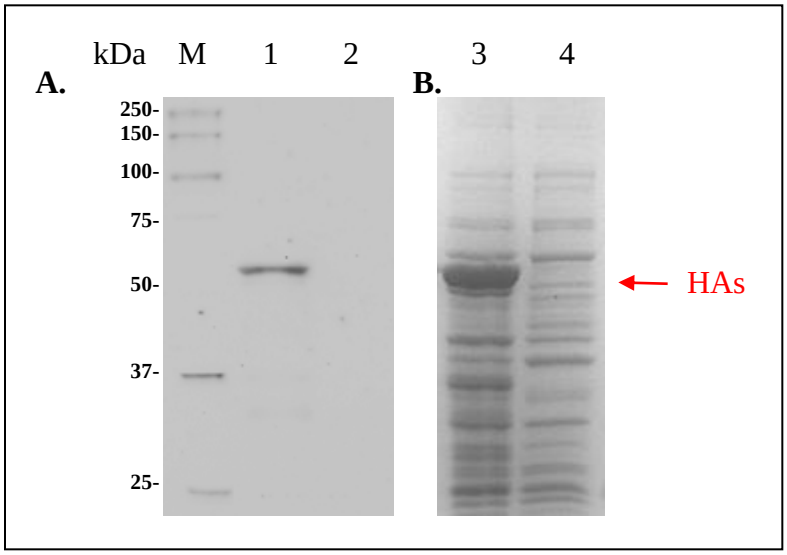

Fig. 3.5. Comfirmation of HAs expression in recombinant DH5α/pTAHAs. A) Western blotting assay; B) SDS-PAGE assay; Lane: M, Protein ladder; 1, recombinant DH5α/pTAHAs 3.5 h after induction (pellet, insoluble fraction, 10 fold dilution); 2, recombinant DH5α/pTAHAs without induction 3.5 h after IPTG was added to another sample; 3, recombinant DH5α/pTAHAs after induction (pellet, insoluble fraction); 4, recombinant DH5α/pTAHAs without induction 3.5 h after IPTG was added to another sample. The proteins were separated by 10% SDS-PAGE gel.

To further confirm that the HAs was expressed as insoluble protein, we conducted Western Blot assay. The mouse anti-HA antibody was applied as primary antibody and anti-mouse IgG HRP conjugated antibody was applied as secondary antibody to detect HAs as described in 2.3.3. There was only one band in Fig. 3.5 (A), which revealed that the proteins expressed in the inclusion bodies were HAs. Also, same as the results we observed in SDS-PAGE assay, there was no HAs protein in the soluble fraction of the collected sample. HAs specific antibody only recognized certain epitopes of HA protein, therefore the fact that the band S observed in Fig. 3.4.did not appear in Fig. 3.5 (A) did not exclude its possibility to be degraded parts of HAs.

3.3. Purification of HAs proteins

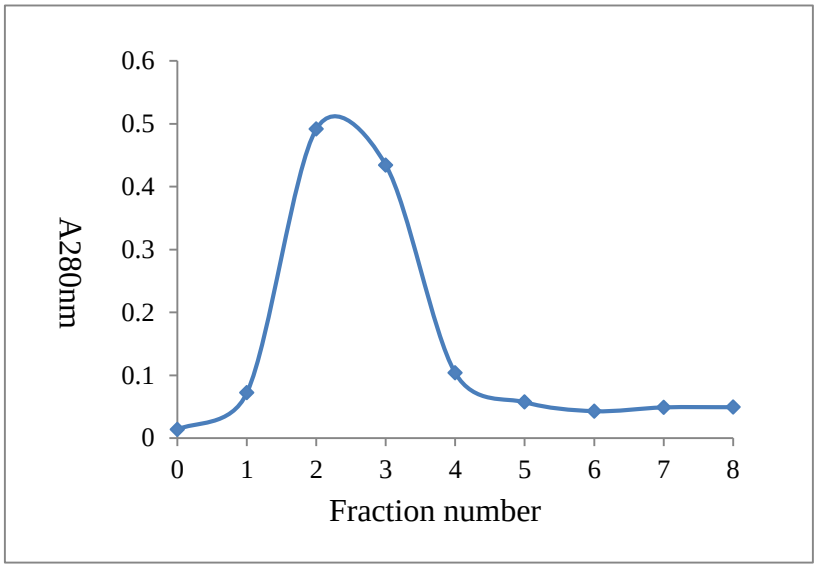

Fig. 3.6. Elution pattern of HAs from Ni-NTA column. The recombinant proteins with His-tag were eluted from the NTA-Ni column under pH 5.0. Lane 0. Wash fraction; Lane 1-8, elute fraction (1ml/tube). The peak of absorbance appeared between fraction 2 and 3 which indicates that large amount of HAs were eluted from the column.

After confirmation of the expression of HAs in *E.coli* cells, we worked on the purification of this recombinant protein. Culture of large volume (400-500ml) was incubated and IPTG was added to a final concentration of 0.1mM when the cell density reached OD_{600}=0.6. All the culture 3.5 h post induction was collected and the soluble fraction was removed by B-PER II bacterial protein

extraction reagent as mentioned in 2.3.2. The inclusion bodies left in the insoluble fraction were broken by 8 M urea (buffer B, pH 8.0) to release the insoluble proteins which contains HAs.

Tubes (1.5 ml) were prepared to collect each fraction during the purification (1 ml/tube). Before applying to the affinity column, the sample was filtered to remove any insoluble part that might block the column and affect the yield and purity of the final product. The filtered sample was then loaded to a pre-equilibrated column filled with 1ml Ni-NTA resin at a low speed (0.2 ml/min) to make sure that HAs with His-tag have enough time to bind Ni chelated on the NTA. Afterwards, around 10ml buffer B was applied to wash away the unbound proteins. 30-40 ml washing buffer (pH 6.3) was applied to the column until the A_{280} was below 0.01. The elution step also needed to be conducted very slowly. Eight fractions with 1ml each were collected after applying buffer D (pH 5.0). The appearance of proteins with His-tag was detected by measuring absorbance at 280 nm. In Fig. 3.6., the absorbance patter of eluted fraction had a peak with a value over 0.5 between fraction 2 and 3. This result indicated that large quantity of HAs were eluted in these two fractions.

To further check the purity of the eluted HAs, a partial of 20 µl of the flow-through (FT), the wash fraction (W) and each elute fraction (E1-E6) were applied for SDS-PAGE assay. As shown in Fig. 3.7., bright bands with the size of HAs appeared in fraction 2 and 3. The proteins in FT were proteins which do not have His-tag so that they could not bind with the Ni-NTA resin. With the decrease of pH value of the buffers, the binding capability of proteins without His-tag decreases as well. Thus, the washing step removed the proteins weakly bound to the resin because of continuous appearance of His in its protein sequences which exposed to the outside. As shown in W, most of the unspecific binding proteins were eliminated, even few HAs proteins

were washed away from the column. In general, we obtained HAs with high purity after purification under denaturing conditions.

Immediately after the completion of purification, we mixed the elution fraction besides the first one which contain few wash fraction. To avoid the occurrence of protein precipitation during dialysis, the average A_{280} of the mixture was adjusted to 0.1 by adding extra buffer D. Buffers with different concentration of urea were prepared in advance as described in 2.4.3. The denatured HAs proteins were refolded during the process to remove the urea in the buffer. In the final step of dialysis, the solution of refolded HAs was replaced by 0.9% NaCl containing 25 mM Tris-HCl (pH 7.5) for future use in animal immunization. Because the volume of vaccine mixture could be injected into mice intramuscularly was limited, we concentrated the dialyzed proteins by Amicon size-cut filter tubes. During this process, proteins of size smaller than up to 30kDa would be removed. As a result, the purity of the HAs was improved again. Finally, we could collect ~250μg recombinant HAs from 500ml initial bacterial culture.

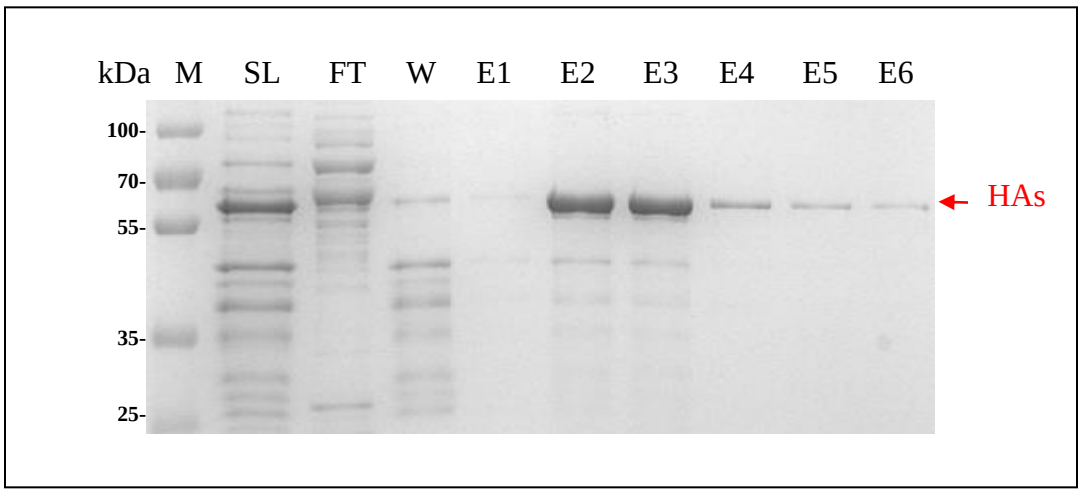

Fig. 3.7. SDS-PAGE assay of eluted HAs from Ni-NTA column. Lane: M, protein ladder; SL, 5× diluted loading sample; FT, 2× flow through; W, wash fraction; E1-6, elution fractions. The HAs were eluted mainly at fraction 2 and 3 which accords with the absorbance pattern.

3.4. Conjugation of HAs with ION

To confirm that the recombinant HAs were bound to the nanoparticles prepared by Ocean Nanotech LLC, the mixture of 4.4 ng SHT (IO-NTA-Ni) and 1.25 μg HAs protein at 4°C for 2 h (nIO:nProtein=1:5 as suggested by company) was loaded to 1% agarose gel for electrophoresis; 4.4 ng SHP (IO-COOH) was also mixed with 1.25 μg HAs protein as negative control.

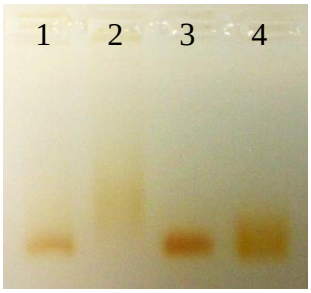

Fig. 3.8. Agarose gel electrophoresis analysis of HAs protein conjugated to IO-NTA-Ni nanoparticle (Ocean Nanotech). Lane 1-4, 1% Agarose gel, (Lane 1) SHT, (Lane 2) SHT mixed with HAs proteins, (Lane 3) SHP and (Lane 4) SHP mixed with HAs proteins.

In Fig. 3.8, Lane 2 showed that SHT conjugated with HAs proteins were evenly distributed on the gel above the position of SHT only. The binding of HAs increased the size of the nanoparticles and decreased the positive charge of the nanoparticles. It is noted that in lane 4, SHP had a few unspecific binding with HA proteins as well. Therefore, HAs were successfully bound to IO-NTA-Ni in a solution containing 10 mM Tris-HCl, 0.1 M NaCl, pH 7.5.

During the preparation of vaccination, we also quantified the HAs loaded onto SHT. The HAs loading efficiency of SHP was determined indirectly by comparison of protein concentration before and after conjugation reaction detected by BCA assay. The quantification of the loaded HAs was calculated using the following equation:

$$\text{Protein loading efficiency (mg/mg)} = (C_{p1} \times V_1 - C_{p2} \times V_2) / (C_{p1} \times V_1)$$

C_{p1} is the concentration of initial concentrated HAs proteins with an initial volume (V_1) added to the mixture. C_{p2} is the concentration of the free HAs proteins in the filtration liquid of a filtration volume (V_2). After filtration, few free HAs left in the filtration liquid, and the loading efficiency is ~90% after calculation.

3.5. Detection of humoral immunity in immunized mice

3.5.1. The symptoms of experimental mice

The injections were performed at around 5-6 pm of a day (routes shown in Fig. 3.9 (A)). The seven-week-old mice were always very active at this time. A mouse was restrained by single hand and the other hand performed the injection. After being restrained, most of the mice had accelerated breathing accompany with slight trembling. It was very frequent that they excreted during the injection. Few mice kicked or struggled, which may because the tip of the needle touched their femur or sciatic nerves, which should be avoided. The activity of the mice was relatively decreased and they were easy to be scared after the injection, but no intumescence or allergy was observed at the injection site. Ten days after each injection, blood samples were collected from submandibular vein.

During bleeding, the strength used to hold the skin on the back of the mouse's neck may influence the localization of the correct bleeding site. Under very few circumstances, the blood came out from the mouse's ear because the puncture was a little bit high towards the ear. The excessive loss of blood caused severe convulsions and distinct decline of activity in one mouse. After received a subcutaneous injection of saline solution at the base of a fold of loose skin (area at the neck), the mouse behaved normally next day.

Serum is the blood plasma with the fibrinogens removed and contains neither any blood cells nor clotting factor. As for the separation of serum from the coagulated blood sample, sometimes its

color was orange red instead of light yellow due to the occurrence of hemolysis (break of red cells). From the results of ELISA which will be presented later, the leak of red blood cells did not influence the detection of HA-specific antibodies.

The weight of mice was monitored every another day at around 5-6 pm. Depends on various conditions of diet and excretion of each mouse at that moment, its weight was not stable. Still, the tendency of weight indicates the basic health status of the mice after immunization. As shown in Fig. 3.9 (B), their weights maintained within 98.3%-112.4% of original weights, without apparently changes.

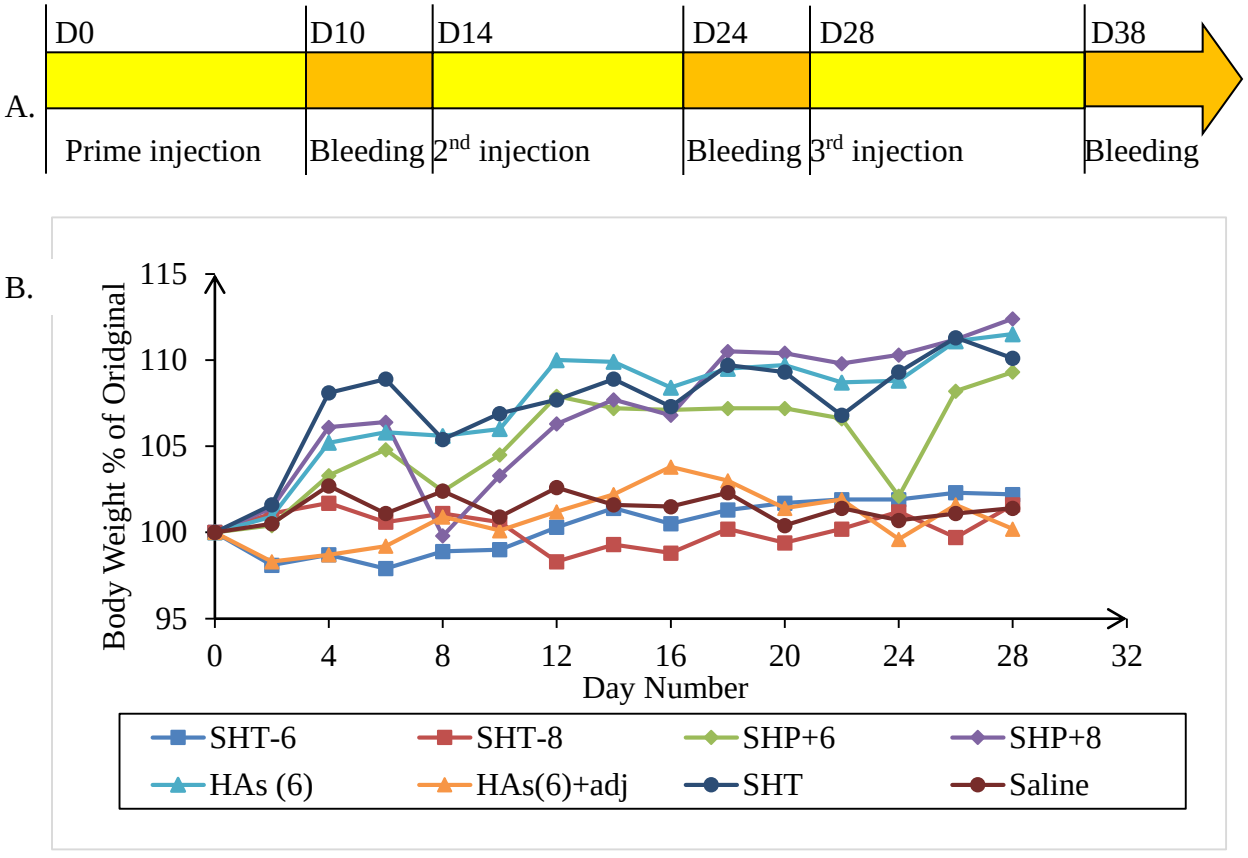

Fig. 3.9. A. The route of administration of nano-vaccines in mice. Groups of Balb/c mice were immunized every two weeks and the blood samples were collected ten days post each immunization. **B. Mice weight tendency.** The body weight of every another day was compared with original weight of each individual mouse.

3.5.2. Immunogenicity of nano-vaccine tested in mice

The HA-specific antibodies titers generated in different groups of immunized mice were detected using ELISA. The results of preliminary experiments showed that mice immunized with SHT binding with 2 μg or 4 μg HAs did not elicit the production of anti-HA IgG until the second boost immunization and average $\log_2$ titers of the generated IgG were very low (< 4), which indicated that the doses of 2 μg or 4 μg were not sufficient to elicit effective humoral immune response in immunized mice. Thus, here we analyzed the results of the latter experiments (data listed in table 3.1). Two weeks after the second boost immunization, HA-specific antibodies were detected in all the immunized groups except for those injected with saline and SHT (Fig. 3.10). The generation of HA-specific antibodies also indicated that an increasing humoral immune response was stimulated in experimental mice after vaccination.

Groups	**HA-specific $\log_2$ titer**		
	Prime	**Boost**	**Second boost**
Saline	0.00±0.00	0.00±0.00	0.00±0.00
SHT	0.00±0.00	0.67±0.58	1.00±1.00
HAs-6	0.67±1.15	3.00±1.00	6.00±2.64
SHT-6	0.00±0.00	2.33±1.53	6.67±3.51
SHT-8	0.00±0.00	1.67±1.15	5.67±2.08
SHP-6	0.00±0.00	1.67±1.15	3.67±2.52
SHP-8	0.00±0.00	1.67±0.58	6.33±1.53
HAs6-adj	1.67±0.58	8.67±0.58	12.00±0.00

Table 3.1. Mean $\log_2$ titers of HA-specific antibodies generated in mice of each group.

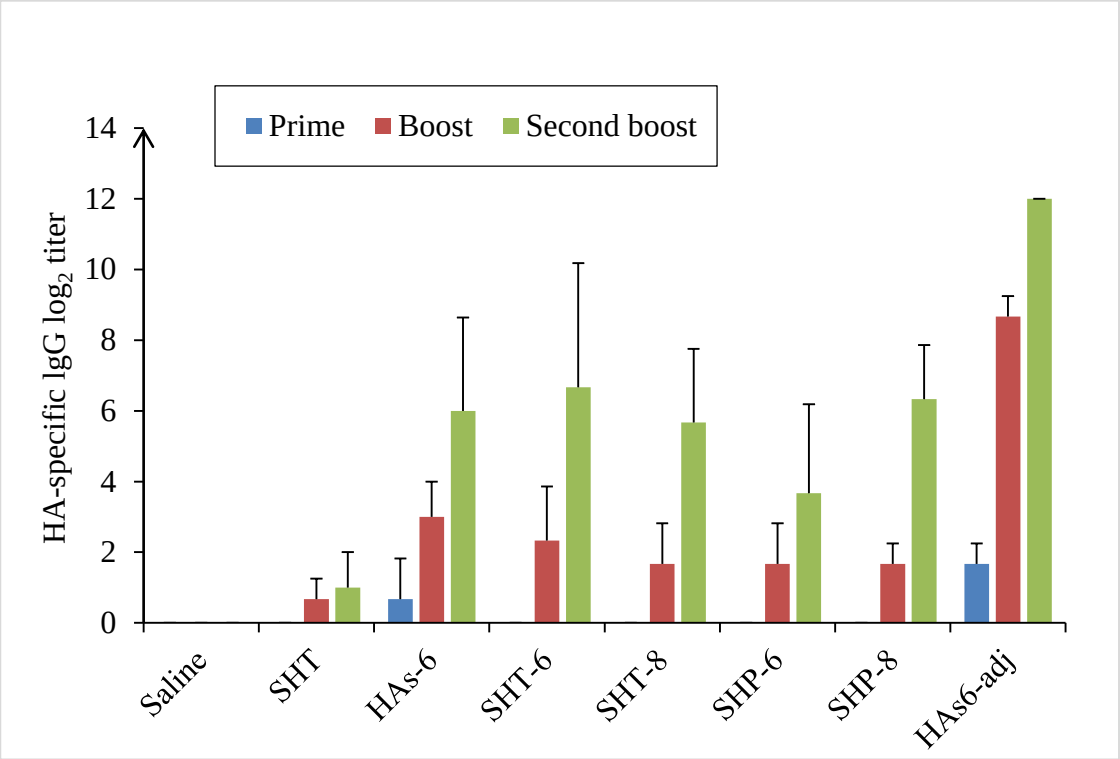

Fig. 3.10. ELISA for HA-specific IgG elicited in immunized mice. Sera from three mouse per group were collected ten days post each immunization and analyzed for the production of anti-HA IgG via ELISA. Antibody titers are expressed as the $\log_2$ values of the endpoint titers. Mice were immunized intramuscularly with 50µl mixture containing 6 µg/8 µg recombinant HAs conjugated with SHT (SHT-6/SHT-8), those mixed with SHP (SHP-6/SHP-8) or those emulsified with CFA/IFA (HAs6-adj). Mice were also immunized intramuscularly with 50µl solution containing 6µg recombinant HAs only (HAs-6), SHT or saline. Error bars, SD, n=3.

Because the number of repeat in each group was relatively small, the individual differences were relatively large in the results. As a result, although SHT-6 showed a higher mean titer than HAs6, its titer was not significantly higher than that of HAs6 at a 95% confidence interval, which indicates that the conjugation of 6 µg HAs to SHT did not enhance the HA-specific antibody responses in immunized mice. Similarly, although SHP-6 showed a lower mean titer than SHT-6, its titer was not significantly lower than that of SHT-6 at a 95% confidence interval. This result suggests that the binding of ION with HAs or not did not influence the production of anti-HA

antibodies in immunized mice. The increase of doses did not significantly improve the antibody titer in SHT-6 and SHT-8, but in SHP-6 and SHP-8. On the other hand, 6 μg HAs emulsified with CFA/IFA stimulated significant higher titer of anti-HA antibodies in immunized mice after the second boost immunization. The statistical significant difference analysis was presented in Table 3.2.

Groups	**HA-specific log_2 titer**			
	Mouse 1	**Mouse 2**	**Mouse 3**	**Mean ± SD[p]**
HAs-6	7	3	8	$6.00\pm2.64^{a,b,c}$
SHT-6	7	3	10	$6.67\pm3.51^{a,d,e}$
SHT-8	8	4	5	5.67 ± 2.08^{d}
SHP-6	6	1	4	$3.67\pm2.52^{b,e,f}$
SHP-8	8	5	6	$6.33\pm1.53^{f**}$
HAs6-adj	12	12	12	$12.00\pm0.00^{c*}$

Table 3.2. Significant comparison between HA-specific IgG elicited in different groups of immunized mice after second boost immunization. P value of paired student t-test: a=0.211, b=0.059, c=0.030, d=0.333, e=0.094, f=0.029.* Significantly higher (P< 0.05) than antibody titer of HAs-6. ** Significantly higher (P< 0.05) than antibody titer of SHP-8.

We expected that the average log_2 titers of anti-HA IgG could reach 12~15 in mice immunized with nano-vaccines or HAs emulsified with CFA/IFA after second boost immunization as shown in Pusic K's work (58), but the nano-vaccines did not improve the HA-specific antibody production to this level in immunized mice. Many factors may cause the experimental results not consistent with our assumptions. First, the amount of HAs in nano-vaccines may be overestimated. The BCA assay reflected the total amount of purified proteins, which included few impurity. Besides, degradation of HAs may happen during different steps of vaccine

preparation, such as the conjugation with IONs, and the removal of unbounded HAs by centrifugal filter. Degradation can also occur during the delivery of vaccines before immunizing the mice. Each possibility may lead to a reducing amount of active antigens in the nano-vaccines, so there is not sufficient dose of HAs together with IONs to produce comparable level of HA-specific antibodies as those emulsified with CFA/IFA. To solve these problems, we can handle higher dose of HAs; we can also modify the condition of purification and dialysis to protect the proteins from degradation. Second, the IONs may not be efficiently captured by APCs to make HAs "visualized" by the immune system of mice. Particle size is very important for antigen uptake by APCs and routes of the CD4+ T cell response (59; 60). The particles investigated in this study are of a size of 10 nm, entering APCs by receptor-mediated endocytosis together with HAs. The enzymes in endosome will detach the conjugation between IONs and HAs, and process the proteins into peptides. We can replace the IONs with those of larger diameters or additional surface modification to enhance their targeting to APCs. Third, imperfect operation in animal immunization may affect the accuracy of the results. Antibody plays significant function in adaptive immunity as blocking virus binding and entry into host cells, therefore, we evaluate the immunogenicity of each vaccine by measuring the level of generated HA-specific antibody in immunized mice. However, intramuscular injection demands experienced handling, and slight variation of the injected volume is easy to take place. Also, the vaccine preparation may not be mixed thoroughly before injection, so the HAs together with IONs are not distributed evenly in the mixture. All of these factors may lead to poor repeatability of the HA-specific antibody titers of mice in the same group, which impacts the significant analysis of these data. To compensate errors resulted from these reasons, we should increase the number of animals in each group.

IV. CONCLUSIONS AND FUTURE WORKS

The HA glycoprotein is considered as a key target for both cellular and humoral immune response against influenza virus. In this study we reported the sub-cloning and expression of HAs from a H5N1 influenza virus in *E.coli*. Our experimental results suggested that the glycosylation is not necessary for recombinant HAs to elicit humoral immune response in immunized mice, and the *E.coli* expression system is able to produce subunit HAs vaccine against influenza virus. We also showed that the HAs is expressed as early as at 0.5 h post induction, and reaches highest expression level between 3.5-4.5 h after the addition of inducer IPTG. The expression of HAs brings growth pressures to the bacterial cells. Using the purification and refolding methods developed in this study, we collected recombinant HAs protein from the bacterial culture at a yield of 250 µg/500 ml. Later, we demonstrated that the concentrated HAs proteins are able to bind with SHT (ION-NTA-Ni) nanoparticles at a high loading ratio ~90%. In the animal studies, we found that 6 µg recombinant HAs was sufficient to stimulate increasing production of HA-specific IgG in mice post three-time immunization. Meanwhile, we noticed that HAs conjugated with SHT did not perform significant improvement of HA-specific antibody production in immunized mice, compared with HAs.

Future works need to be focused on the modification of nano-vaccines in order to continue the investigation of IONs as potential delivery platform of influenza vaccine. On one hand, we could improve the activity of recombinant HAs by optimizing conditions of dialysis, conjugation with IONs and vaccine preservation to reduce the protein degradation. We could also modify the IONs by increasing their diameter or attaching molecules that facilitate APC targeting to their surface. On the other hand, we could keep exploring the immunogenicity of current vaccine preparation carrying higher dose of HAs. ELISA in this study only detected the generation level

of total IgG, which peaks 4-6 weeks after natural infection. Subtypes of IgG could be further detected in order to determine what type of them dominates in the humoral immune responses of immunized mice. Long-term immune protection provided by the nano-vaccine can be detected on the sera collected half a month or longer post the second boost injection. Although we anticipated that conjugation of HAs with IONs could enhance the humoral immune responses in mice, IONs may augment the cellular immune responses instead. Enzyme-linked immunosorbent spot assay (ELISPOT) will be performed to measure the increase number of IFN-γ-secreting T cells from freshly collected splenocytes of immunized mice. The same assay could be applied to detect HA-specific interleukin-12 (IL-12) or interleukin-4 (IL-4) production in immunized mice, which indicate whether the IONs activate the CD4+ T cells via Th1 or Th2 route. The HA-specific antiviral CD8+/cytotoxic T cell (CTL) responses can be characterized by chromium [51Cr]-release assay.

After modification of the nano-vaccines from different aspects as mentioned above, we expect that mean $\log_2$ titers of anti-HA IgG could be higher than 13 in mice immunized with nano-vaccines. Because high total IgG level does not guarantee that sufficient protective antibodies against virus strain are elicited in immunized mice, we will perform the hemagglutination inhibition (HI) assay to determine functional anti-HA antibody titer. Also, we could perform *in vitro* microneutralization (MN) assay, a highly sensitive and specific assay, to measure the serum neutralizing capacity against the homologous H5N1 influenza virus in immunized mice before moving forward to the assessment of their functional protective efficacy by host challenge against H5N1 strain.

REFRENCES

1. Centers for Disease Control and Prevention. Epidemiology and Prevention of Vaccine-Preventable Diseases. Atkinson W, Wolfe S, Hamborsky J, eds. 12th ed., second printing. Washington DC: Public Health Foundation, 2012.

2. Suarez DL, Schultz-Cherry S (2000) Immunology of avian influenza virus: a review. *Dev Comp Immunol* 24:269-283.

3. Hay AJ, Gregory V, Douglas AR, Lin YP (2001) The eveloution of human influenza viruses. *Philos Trans R Soc Lond B Biol Sci* 356:1861-70.

4. Nicholson KG, Wood JM, Zambon M (2003) Influenza. *Lancet* 362:1733-45.

5. Crawford J, *et al.* (1999) Baculovirus-derived hemaggluinin vaccines protect against lethal influenza infections by avian H5 and H7 subypes. *Vaccine* 2265-2274.

6. Kozlowski L (2007-2012) Isoelectric point Calculator. [Online] http://isoelectric.ovh.org.

7. Subbarao K, *et al.* (1998) Characterization of an avian influenza A (H5N1) virus isolated from a child with a fatal respiratory illness. *Science* 279: 393-396.

8. Taubenberger JK, Morens DM (2006) 1918 Influenza: the mother of all pandemics. *Emerg Infect Dis* 12: 15-22.

9. WHO (2012) H5N1 avian influenza: Timeline of major events. [Online] http://www.who.int/influenza/H5N1_avian_influenza_update_20121217b.pdf.

10. WHO (2013) Cumulative number of confirmed human cases for avian influenza A (H5N1) reported to WHO, 2003-2013. [Online] http://www.who.int/influenza/human_animal_interface/EN_GIP_20131008CumulativeNumberH5N1cases.pdf.

11. Salhanick M (2013) Ethical considerations for NIH funded highly transmissible H5N1. *Pharos Alpha Omega Alpha Honor Med Soc* 76:7-9.

12. WHO (2013) Antigenic and genetic characteristics of zoonotic influenza viruesse and the development of candidate vaccine viruses for pandemic preparedness. [Online] http://www.who.int/influenza/vaccines/virus/201309_h5h7h9_vaccinevirusupdate.pdf.

13. Giudice GD, Fragapane E, Cioppa GD, Rappuoli R (2013) Aflunov: a vaccine tailored for pre-pandemic and pandemic approaches against influenza. *Expert Opin Biol Ther* 13: 121-135.

14. WHO (2011) Report of the 7th meeting on evaluation of pandemic influenza vaccines in clinical trials, world health organization, Geneva, 17-18 February 2011. *Vaccine* 29:7579-7586.

15. Wang KY, *et al.* (2006) Expression and Purification of an influenza hemagglutinin-one step closer to a recombinant protein-based influenza vaccine. *Vaccine* 24: 2176-2185.

16. Shaw A (2012) New technologies fro new influenza vaccines. *Vaccine* 30:4927-4933.

17. Normile D (2004) WHO Ramps Up Bird Flu Vaccine Efforts. *Science* 303: 609.

18. Brands R, *et al.* (1999) Influvac: a safe Madin Darby Canine Kidney (MDCK) cell culture-based influenza vaccine. *Dev Biol Stand* 98:93-100.

19. Percheson PB, Trepanier P, Dugre R, Mabrouk T (1999) A Phase I, randomized controlled clinical trial to study the reactogenicity and immunogenicity of a new split influenza vaccine derived from a non-tumorigenic cell line. *Dev Biol Stand* 98:127-132.

20. Alymova IV, *et al.* (1998) Immunogenicity and protective efficacy in mice of infleunza B virus vaccines grown in mammalian cells or embryonated chicken eggs. *J Virol* 72:4472-7.

21. Robertson JS, *et al.* (1985) Alteratuions in the hemagglutinin associated with adaptation of influenza B virus to growth in eggs. *Virology* 143:166-174.

22. Schild GC, Oxford JS, de Jong JC, Webster RG (1983) Evidence for host cell selection of influenza virus antigenic variants. *Nature* 303:706-709.

23. Ulmer JB, Sadoff JC, Liu MA (1996) DNA vaccines. *Curr opin Immunol* 8:531-536.

24. Gurunathan S, Wu CY, Freidag BL, Seder RA (2000) DNA vaccines: a key for inducing long-term cellular immunity. *Curr opin Immunol* 12:442-447.

25. Ledgerwood JE, *et al.* (2012) Influenza virus H5 DNA vaccination is immunogenic by intramuscular and intradermal routes in humans. *Clin Vaccine Immunol* 19:1792-1797.

26. Gao WT, *et al.* (2006) Protection of mice and poultry from lethal H5N1 avian influenza virus through adenovirus-based immunization. *Virology* 1959-1964.

27. Cox MMJ (2012) Recombinant protein vaccines produced in insect cells. *Vaccine* 30:1759-1766.

28. Khurana S, *et al.* (2011) H5N1 virus-like particle vaccine elicits cross-reactive neutralizing antibodies that preferentially bind to the oligomeric form of influenza virus hemagglutinin in humans. *J Virol* 85:10945-10954.

29. Khurana S, *et al.* (2011) Bacterial HA1 Vaccine against Pandemic H5N1 Influenza Virus: Evidence of Oligomerization, Hemagglutination, and Cross-Protective Immunity in Ferrets. *J Virol* 85: 1246-1256.

30. Kang SM, Song JM, Compans RW (2011) Novel vaccines against influenza viruses. *Virus Res* 162: 31-38.

31. Sasaki S, Okuda K (2000) The use of conventional immunologic adjuvants in DNA Vaccine Preparations. *Methods Mol Med* 29:241-249.

32. Kenney RT, Edelman R (2003) Survey of human-use adjuvants. *Expert Rev Vaccines* 2:167-188.

33. Robert LH (2002) Overview of vaccine adjuvants: present and future. *Vaccine* 20:S7-S12.

34. Amand LG (2006) Adjuvant-enhanced antibody responses occur without Toll-like receptor signaling. *Science* 314: 1936-1938.

35. Brewer JM, *et al.* (1999) Aluminium hydroxide adjuvant initiates strong antigen-specific Th2 responses in the absence of IL-4-or IL-13-mediated signaling. *J Immunol* 163: 6448-6454.

36. Reed SG, Bertholet S, Coler RN, Friede M (2008) New horizons in adjuvants for vaccine development. *Trends immunol* 30:23-32.

37. Khurana S, *et al.* (2010) Vaccines with MF59 Adjuvant Expand the Antibody Repertoire to Target Protective Sites of Pandemic Avian H5N1 Influenza Virus. *Sci Trans Med* 2:15ra5.

38. Radosevic K, *et al.* (2008) Antigody and T-cell responses to a virosomal adjuvanted H9N2 avian influenza vaccine: impact of distinct additional adjuvants. *Vaccine* 26:3640-3646.

39. Clegg CH, *et al.* (2012) Adjuvant solution for pandemic influenza vaccine production. *PNAS* 109:17585-17590.

40. Oyewumi MO, Kumar A, Cui Z (2010) Nano-microparticles as immune adjuvants: correlating particle sizes and the resultant immune responses. *Expert Rev Vaccines* 9:1095-1107.

41. Klippstein R, Pozo D (2010) Nanotechnology-based manipulation of dendritic cells for enhanced immuotherapy strategies. *Nanomedicine* 6:523-529.

42. Kreuter J (2000) Poly(Methyl Methacrylate) nanoparticles as vaccine adjuvants. *Methods Mole Med* 42:105-119.

43. Akerman ME, Chan WC, Laakkonen P, Bhatia SN, Ruoslahti E (2002) Nanocrystal targeting in vivo. *PNAS* 99:12617-12621.

44. Fahmy TM, Demento SL, Caplan MJ, Mellman I, Saltzman WM (2008) Design opportunities for actively targeted nanoparticle vaccines. *Nanomedicine* 3:343-355.

45. Roy I, Vij N (2010) Nanodelivery in airway diseases: Challenges and therapeutic applications. *Nanomedicine* 6:237-244.

46. Shahiwala A, Vyas TK, Amiji MM (2007) Nanocarriers for systemic and mucosal vaccine delivery. *Recent Pat Drug Deliv Formul* 1:1-9.

47. Bharali DJ, *et al.* (2008) Novel nanoparticles for the delivery of recombinant hepatitis B vaccine. *Nanomedicine* 4:311-317.

48. Tang J, *et al.* (2012) A novel self-assembled nanoparticle vaccine with HIV-1 Tat(49-57)/HPV16 E7(49-57) fusion peptide and GM-CSF DNA elicits potent and prolonged CD8(+) T cell-dependent anti-tumor immunity in mice. *Vaccine* 30:1071-1082.

49. Kaba SA, *et al.* (2012) Protective antibody and CD8+ T-cell responses to the Plasmodium falciparum circumsporozoite protein induced by a nanoparticle vaccine. *PLoS One* 7:e48304.

50. Rodriguez PL, *et al.* (2013) Minimal "self"peptides that inhibit phagocytic clearance and enhance delivery of nanoparticles. *Science* 339: 971-975.

51. Weissleder R, *et al.* (1989) Superparamagnetic iron oxide: pharmacokinetics and toxicity. *AJR Am J Roentgenol* 152:167-173.

52. Faraji M, Yamini Y, Rezaee M (2010) Magnetic Nanoparticles: Synthesis, Stabilization, Functionalization, Characterization, and Applications. *J Iran Chem Soc* 7:1-37.

53. Foy SP, *et al.* (2010) Optical Imaging and Magnetic Field Targeting of Magnetic Nanoparticles in Tumors. *ACS Nano* 4: 5217-5224.

54. Kievit FM, *et al.* (2012) Targeting of Primary Breast Cancers and Metastases in a Transgenic Mouse Model Using Rationally Designed Multifunctional SPIONs. *ACS Nano* 6: 2591-2601.

55. Corsi F, *et al*. (2011) HER2 Expression in Breast Cancer Cells Is Downregulated Upon Active Targeting by Antibody-Engineered Multifunctional Nanoparticles in Mice. *ACS Nano* 5: 6383-6393.

56. Farrell D, *et al.* (2010) Recent Advances from the National Cancer Institute Alliance for Nanotechnology in Cancer. *ACS Nano* 4: 589-594.

57. Zaks TZ, Rosenberg SA (1998) Immunization with a peptide epitope (p369-377) from HER-2/neu leads to peptide-specific cytotoxic T lymphocytes that fail to recognize HER-2/neu+ tumors. *Cancer Res* 58:4902-4908.

58. Pusic K, *et al.* (2013) Iron oxide nanoparticles as a clinically acceptable delivery platform for a recombinant blood-stage human malaria vaccine. *FASEB J* 27: 1153-66.

59. Navrotsky A, Mazeina L, Majzlan J (2008) Size-driven structural and thermodynamic complexity in iron oxides. *Science* 319: 1635-1638.

60. Fifis T, *et al.* (2004) Size-dependent immunogenicity: Therapeutic and protective properties of nano-vaccines against tumors. *Journal of Immunology* 173: 3148-3154.

61. Levine MM. (2010) Immunogenicity and efficacy of oral vaccines in developing countries: lessons from a live cholera vaccine. *BMC Biol* 8: 129-139.

62. Clercq E De (2006) Antiviral agents active against influenza A viruses. *Nat Rev Drug Discov* 5, 1015-1025.

63. Belshe R, *et al*. (2005) The origins of pandemic influenza-lessons from the 1918 virus. *N Engl J Med* 353: 2209–2211.

64. Hatibi I, *et al*. (2013) The fast diagnosis by different methodologies of the influenza virus. *Albanian J Agric Sci* 12: 445-448.

65. Nelson MI, Holmes EC (2007) The evolution of epidemic influenza. *Nat Rev Genet* 8: 196-205.

66. Hilleman MR (2002) Realities and enigmas of huam viral influeza: pathogenesis, epidemiology and control. *Vaccine* 20: 3068-3087.

67. Murphy FA (1973) [Online] http://phil.cdc.gov/phil/details.asp?pid=8432.

68. Amorij J-P, *et al*. (2008) Development of stable influenza vaccine prowder formulations: challenges and possiblities. *Pharm Res* 6:1256-1273.

APPENDIX

6.1 Approval letter of IACUC protocol

UNIVERSITY OF ARKANSAS

Office of Research Compliance

MEMORANDUM

TO: Kaiming Ye

FROM: Craig N. Coon, Chairman
Institutional Animal Care
And Use Committee

DATE: June 20, 2013

SUBJECT: IACUC Protocol **APPROVAL**
Expiration date : **June 16 , 2016**

The Institutional Animal Care and Use Committee (IACUC) has **APPROVED** Protocol **#13056 - "Development of a Nano-vaccine against H5N1 Influenza"**. You may begin this study immediately.

The IACUC encourages you to make sure that you are also in compliance with other UAF committees such as Biosafety, Toxic Substances and/or Radiation Safety if your project has components that fall under their purview.

In granting its approval, the IACUC has approved only the protocol provided. Should there be any changes to the protocol during the research, please notify the IACUC in writing [via the Modification Request form] **prior** to initiating the changes. If the study period is expected to extend beyond **06-16-2016** you must submit a new protocol. By policy the IACUC cannot approve a study for more than 3 years at a time.

The IACUC appreciates your cooperation in complying with University and Federal guidelines for research involving animal subjects.

cnc/car

cc: Animal Welfare Veterinarian

Administration Building 210 • 1 University of Arkansas • Fayetteville, AR 72701-1201 • 479-575-4572
Fax: 479-575-3846 • http://vpred.uark.edu/199

6.2 Approval letter of IACUC modification request

UNIVERSITY OF ARKANSAS

Office of Research Compliance

MEMORANDUM

TO: Sha Jin

FROM: Craig N. Coon, Chairman
Institutional Animal Care
And Use Committee

DATE: September 10, 2013

SUBJECT: IACUC Modification Request **APPROVAL**
Expiration date : **June 16, 2016**

The Institutional Animal Care and Use Committee (IACUC) has **APPROVED** the modification request (to change the PI) to Protocol **#13056 - "Development of a Nano-vaccine against H5N1 Influenza"**. You may implement this Modification immediately.

The IACUC encourages you to make sure that you are also in compliance with other UAF committees such as Biosafety, Toxic Substances and/or Radiation Safety if your project has components that fall under their purview.

In granting its approval, the IACUC has approved only the protocol/modification provided. Should there be any additional changes in the protocol during the research, please notify the IACUC in writing [via the Modification Request form] **prior** to initiating the changes.

The IACUC appreciates your cooperation in complying with University and Federal guidelines for research involving animal subjects.

cnc/car

cc: Animal Welfare Veterinarian

Administration Building 210 • 1 University of Arkansas • Fayetteville, AR 72701-1201 • 479-575-4572
Fax: 479-575-3846 • http://vpred.uark.edu/199